國立台灣大學醫學學院分子醫學研究所

碩士論文

Graduate Institute of Molecular Medicine

College of Medicine

National Taiwan University

Master Thesis

蛋白酶體活性與 Wnt 訊息傳導路徑調控果蠅神經元

樹突修剪之研究

Roles of Proteasome Activity and Wnt Signaling

Regulation during Neuronal Dendrite Pruning

in *Drosophila*

柯建銘

Jian-Ming Ke

指導教授：李秀香 助理教授

Advisor: Hsiu-Hsiang Lee, Ph.D

中華民國 103 年 12 月

December, 2014

國立臺灣大學碩士學位論文
口試委員會審定書
蛋白酶體活性與 Wnt 訊息傳導路徑調控果蠅神經元
樹突修剪之研究

Roles of Proteasome Activity and Wnt Signaling
Regulation during Neuronal Dendrite Pruning
in *Drosophila*

本論文係柯建銘（R0144014）在國立臺灣大學分子醫學研究所完成之碩士學位論文，於民國 103 年 11 月 20 日承下列考試委員審查通過及口試及格，特此證明

口試委員：

李秀香

（簽名）

（指導教授）

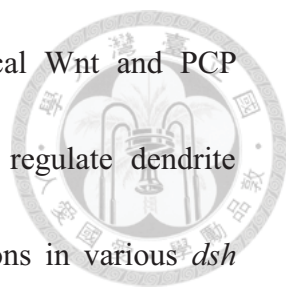徐元中

虞瑞萩

所長　　　　李嘉銘　　（簽名）

1

i

誌謝

Abstract

Neuronal remodeling plays a critical role during development from invertebrates to vertebrates. Pruning, one of the neuronal remodeling mechanisms, is a process to selectively remove specific parts of neurons without causing cell death. In *Drosophila*, the class IV dendritic arborization (da) neurons, which undergo pruning process to eliminate larval dendrites during metamorphosis, is an ideal model system to study the underlying mechanisms of pruning.

Previous studies showed that ubiquitin proteasome system (UPS) initiates the dendrite pruning. To address the dynamics of proteasome activity during pruning process, we generated a photoconvertible reporter system. The decrease of converted fluorescent signals over a period of time could be used to monitor the proteasome activity *in vivo*.

Wingless-Int (Wnt) signaling is crucial for variety of biological events. It could be divided into three major pathways: canonical Wnt pathway, planar cell polarity (PCP) pathway, and calcium pathway. Previous studies reported a trophic role for Wnt-Ror kinase signaling to regulate neuronal pruning in *C.elegans*, thus highlighted the regulatory roles of Wnt signaling. Here, we identified *dishevelled* (*dsh*), a Wnt signaling molecule, as a candidate to regulate *Drosophila* dendrite pruning. Dsh is a

cytoplasmic phosphoprotein, which is involved in both canonical Wnt and PCP pathways. To determine which pathway of Wnt signaling can regulate dendrite pruning, we examined the dendrite pruning of class IV da neurons in various *dsh* mutant flies, and found the canonical Wnt pathway is associated with dendrite pruning. Next, we identified which Wnt receptors might act upstream of *dsh* during dendrite pruning. Consistent with the fact that the redundant roles of *fz* and *fz2* in canonical Wnt signaling, both *fz* and *fz2* loss of function mutants showed pruning defects. Furthermore, a co-receptor *arrow*, which is required for canonical Wnt signaling, also showed some dendrite severing defects when it lost its function. Finally, the canonical Wnt-specific nuclear *TCF* caused critical severing defects when expressing its N-terminal deletion form. Taken together, these results demonstrated that the canonical Wnt pathway is essential for *Drosophila* dendrite pruning.

Keywords: dendrite pruning, class IV da neurons, proteasome activity, Wnt pathway, *dishevelled*, Wnt receptors, *TCF*

摘要

　　從無脊椎動物到脊椎動物，神經元重組(neuronal remodeling)在其生長發育的過程中，都扮演相當關鍵的角色。而在神經元重組的機制裡，其中之一就是修剪(pruning)。在這修剪的過程中，它會選擇性去除掉神經元上特定部分，卻不會導致細胞死亡。以果蠅為例，第四樹突型神經元(class IV da neuron)會在變態這個發育階段中，利用修剪過程來消除幼蟲時期的樹突，因此是作為研究神經元修剪之分子機轉的理想的模式系統。

　　先前的研究發現，泛素-蛋白酶體系統(ubiquitin-proteasome system, UPS)會開啟果蠅神經樹突的修剪。為了瞭解在修剪過程中，蛋白酶體活性的動態變化，我們設計出一個光轉換的報導系統(photoconvertible reporter system)。利用一段時間內被轉換的螢光訊息所降低的量，就可以對活體內的蛋白酶體活性進行監測。

　　Wnt 訊息傳導路徑對生物體中各種生理調控很重要，它可被區分為三種主要的路徑，典型的 Wnt 傳導路徑(canonical Wnt pathway)、平面細胞極性路徑(planar cell polarity pathway, PCP)以及鈣離子路徑(calcium pathway)。先前在線蟲的研究報導發現，Wnt 訊息傳導路徑下的 Ror 激酶可以調控神經元的重組修飾，因而凸顯了 Wnt 訊息傳導路徑在神經元重組過程中的重要性。在此，我們經遺傳篩選(genetic screen)的方式找到了 Wnt 訊息傳導路徑中的成員，即 dishevelled(dsh)這個蛋白，作為可能調控果蠅樹突修剪的候選分子。Dsh 是一種磷酸蛋白，在典型的 Wnt 訊息傳導路徑和平面細胞極性路徑中都有參與。為了找出是哪一種訊息路徑調控神經元樹突的修剪過程，我們檢查各種 *dsh* 突變種果蠅對第四樹突型神經元中樹突修剪的影響，進而發現典型的 Wnt 路徑與樹突修剪的調控有關。接著，我們尋找 dsh 上游的 Wnt 受體，發現在 frizzled(fz)和 frizzled2(fz2)失去功能的突變種之中，的確可以看到樹突修剪上的缺陷。此外我們也找到另一個典型 Wnt 訊息路徑所必需的伴受體 arrow(arr)，當 arr 這個受體蛋白失去功能時，同樣

會導致樹突斷裂(severing)過程上的缺陷。最終，我們表現一種變異型式的 TCF 蛋白，使它原先的氮基端有一段缺失。在這樣的突變種之中，我們同樣觀察到很嚴重的樹突斷裂缺陷。綜合以上結果，我們證明了典型的 Wnt 訊息傳導路徑和調控果蠅樹突修剪的生理過程有關。

關鍵字：神經樹突修剪、第四樹突型神經元、蛋白酶體活性、Wnt 訊息傳導路徑、*dishevelled*、Wnt 受體、*TCF*

Table of Contents

List of Tables

List of Figures

Chapter 1. Introduction

1. Neuronal remodeling

In many kinds of organisms, the nervous system is the most complicated functional architecture. It is primarily composed of neurons and other glial cells. Neurons, the polar cells with axons and dendrites, are the basic functional units of the nervous system. The nerve conduction via axon-dendrites interaction between these neurons orchestrates the overall neural network, which could coordinate multiple signals throughout the whole body of organisms.

To sense the stimuli of external environment accurately, dendrite arbors are often reorganized and refined during different developmental stages. This transformation is called neuronal remodeling. In *Drosophila*, the nervous system undergoes neuronal remodeling during metamorphosis to generate a more complicated neural network that is capable of mediating the distinct behavior of the adult. Among these processes of neuronal remodeling, one could change the amount of neurons through neurogenesis or apoptosis, and another, which we are interested in, could selectively remove specific parts of neurons without causing cell death, referred to as pruning (Kuo et al., 2005).

2. *Drosophila* class IV dendritic arborization (da) neurons
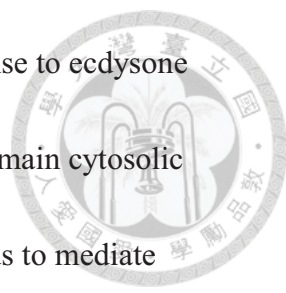
Pruning, one of the neuronal remodeling, is widely observed from invertebrates to vertebrates. In *Drosophila*, the pruning process also occurs both in the central nervous system (CNS) and peripheral nervous system (PNS), including mushroom body γ-neurons (Lee et al., 1999), olfactory projection neurons (Marin et al., 2005) in the CNS, and dendritic arborization (da) neurons (Kuo et al., 2005) in the PNS, respectively.

Drosophila da neurons, which are sensory neurons with extensively branched dendrites cover the epidermis, can be roughly divided into four classes (termed class I - IV) according to their size and complexity of dendritic field (Grueber et al., 2002). These peripheral sensory neurons can detect noxious thermal and mechanical stimuli (Hwang RY et al., 2007) in addition to their recently discovered role as photoreceptors (Xiang Y et al., 2010). During metamorphosis, the stage which *Drosophila* undergoes large-scale neuronal remodeling, most of the da neurons will be dead, whereas class IV da neurons, including ddaC and v'ada, survive and prune their dendrites (Williams et al., 2005). Also, the class IV da neurons have the largest dendritic field, which covers whole the epidermis of the worm body. Thus, *Drosophila* class IV da neurons can be ideal model system to study the mechanism of dendrite pruning.

3. *Drosophila* dendrite pruning

Drosophila dendrite pruning is a tightly controlled process. Four steps of this process could be characterized: severing, fragment, clearance, and regrowth (Williams et al., 2005). At about 5 hours after puparium formation (APF), the primary dendrites would be severed at the proximal sites of class IV da neurons, and gradually detach from the soma. At 10-12 h APF, the severed dendrites would undergo fragmentation, and finally, the debris of these dendrites would be eliminated completely at 16-18 h APF. After the removal step, the class IV da neurons will regrow a more complicated neuronal network which is suitable for adult behavior.

There are many intrinsic and extrinsic factors involved in such pruning process. For intrinsic factors, the steroid hormone ecdysone (Kuo et al., 2005) and the ubiquitin-proteasome system (UPS) (Kuo et al., 2006) initiate the dendrite severing. For extrinsic factors, extracellular matrix metalloproteinase (MMP) is required for severed dendritic debris degradation (Kuo et al., 2005). In addition, Dronc plays a crucial role in the clearance of dendritic debris by phagocytes with its caspase activity (Williams et al., 2006). Katanin p60-like 1 (kat60L1), an AAA-ATPase which facilitates dendritic microtubule disassembly, and Ik2, a serine/threonine kinase which is required for initiation of microtubule severing in dendrites with the kinase activity itself, are both essential for dendrite severing (Lee et al., 2009). Sox14, a transcription

factor, can regulate the expression of the target gene *mical* in response to ecdysone

signaling, and the *mical* gene could subsequently encode a multi-domain cytosolic

protein that is known to associate with cytoskeletal components, thus to mediate

dendrite severing during pruning process (Kirilly et al., 2009). Alongside this, several

molecules have been identified as novel regulators in the pruning pathway, including

the components of the Valosin-containing protein (VCP) (Rumpf et al., 2011),

headcase, a novel target gene of ecdysone signaling (Loncle et al., 2012),

cullin1-based SCF E3 ubiquitin ligase (Wong et al., 2013), and surprisingly, the

compartmentalized calcium transients (Kanamori et al., 2013). Nevertheless, the

relationship between these members is still unclear.

4. Ubiquitin-proteasome system (UPS)

The UPS is the major cytoplasmic proteolytic system. Its molecular function is

critical in transcription, signal transduction, protein quality control, and many other

biological processes (Finley, 2009). This massive molecular machinery serves protein

degradation through a covalent attachment of a poly-ubiquitin chain. It functions by a

cascade of enzymes, including the ubiquitin activating enzyme (E1), the ubiquitin

conjugating enzyme (E2), and the ubiquitin ligase (E3) to conjugate ubiquitin

molecules to the lysine residues of target proteins. In the UPS pathway, E1 activates

an ubiquitin protein first, and this activated ubiquitin is then transferred to E2 via

formation of a thiolester bond. Next, the activated ubiquitin is transferred again to the

substrate to label its fate for destruction by E3 ligase. Finally, after formation of a

poly-ubiquitin chain on the target protein, this protein substrate is destroyed by the

proteasome (Hanna et al., 2007).
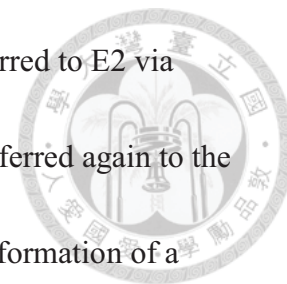
The proteasome, an approximately 2.5MDa protein complex, contains two major

assemblies, the 670kDa 20S core particle (CP) and the 1MDa 19S regulatory particle

(RP). Typically, there are two combinations of CP-RP association, including

single-capped (CP-RP) form and double-capped (RP-CP-RP) form. When the CP is

associated with one or two RP through the axial end of itself, this complex machinery

is referred to as the 26S proteasome.

The 20S CP is a barrel-shaped complex consists of 28 subunits, arranged into

four stacked heteroheptameric rings, which are two outer α rings and two inner β rings.

The outer rings form "α-pockets" to bind the RP, whereas the inner rings contain three

β-type subunits (β1, β2, and β5) to form proteolytic active sites.

The 19S RP, another part of proteasome, can be divided into the base and the lid.

The base sub-complex is located proximal to the CP. It consists of six AAA-type

ATPases (Rpt1-6) and four non-ATPase subunits (Rpn1, Rpn2, Rpn10, and Rpn13).

The Rpt ATPases of the base are critical for CP-RP complex formation, whereas the
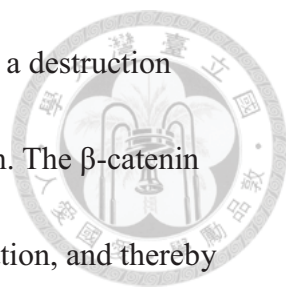
non-ATPase subunits serve as scaffolding proteins (Rpn1 and Rpn2) and the ubiquitin

receptors (Rpn10 and Rpn13). In addition, the lid sub-complex of the RP is located

distal to the base. It is composed of six PCI domain subunits (Rpn3, Rpn5-7, Rpn9,

and Rpn12) and two MPN domain subunits (Rpn8 and Rpn11). The PCI motifs are

through to provide extensive inter-subunit contacts by PCI-PCI interaction, whereas

the MPN domain of Rpn11 contains a metalloprotease-like de-ubiquitinating activity

to remove the ubiquitin molecules from substrates.
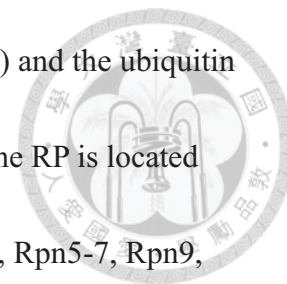
5. Wnt pathways

The Wnt pathway, one kind of signal transduction mechanism, is essential for

variety of biological events. It governs developmental, homeostatic, and pathological

processes through the signal transduction cascade activated by secreted Wnt

morphogens. The Wnt pathways could be roughly divided into canonical, which

means β-catenin-dependent, and non-canonical, a β-catenin-independent signaling.

The canonical Wnt pathway (Wg signaling in *Drosophila*), is that causes the

accumulation of β-catenin in the cytoplasm, and further promotes the translocation of

these accumulated proteins into the nucleus to turn on the Wnt target genes. Without

Wnt stimulation, it mainly regulated by extensive negative control steps. Several

negative regulators, including Axin, adenomatosis polyposis coli (APC), glycogen

synthase kinase 3 (GSK3), and casein kinase 1 (CK1α), would form a destruction

complex assembled by the Axin scaffold, and interact with β-catenin. The β-catenin

would be phosphorylated by GSK3 and CK1, target it for ubiquitination, and thereby

ensuring the degradation by proteasome. However, as soon as the cells exposed to

Wnt signals, these ligands bind Frizzled (fz) and the low-density lipoprotein

receptor-related protein (LRP), a co-receptor of fz, and results the recruitment of the

destruction complex and associated protein Dishevelled (Dsh) to the plasma

membrane. GSK3 and CK1 phosphorylate the cytosolic tail of LRP, and this

phosphorylated tail would bind to Axin. At the same time, Dsh binds fz with its PDZ

domain and binds to Axin with its DIX domain. Subsequently, Axin becomes

de-phosphorylated and de-stabilized. The activity of GSK3 also would be inhibited by

Dsh, thus it cannot phosphorylate β-catenin. As a consequence, the stabilized

β-catenin will be released from the destruction complex, and then translocate into the

nucleus. In the nucleus, T-cell factor/lymphoid enhancing factor (TCF/LEF), which

forms a complex with Groucho and acts as a repressor of Wnt target genes in the

absence of Wnt signals, will be converted into a transcriptional activator by β-catenin,

thus activating the Wnt target genes finally.

　　In the non-canonical pathways, planar cell polarity (PCP) is one of the Wnt

pathways and is β-catenin-independent. The PCP pathway initiates upon the binding

of Wnt to fz, and then the receptor recruits Dsh, which binds to Dishevelled-associated activator of morphogenesis 1 (DAAM1) with its DEP domain to form a complex. Next, Daam1 activates the small G-protein Rho, and the Rho kinase subsequently activates a cytoskeleton regulator, called Rho-associated kinase (ROCK), so that the PCP pathway can regulate planar cell polarity by stimulating cytoskeletal reorganization just as the name it is. In addition, Dsh can also interact with Rac1, and further activate the Rac1-JNK axis to regulate actin polymerization.

The other β-catenin-independent, non-canonical Wnt pathway is calcium pathway. The main function of this pathway is that it can lead to calcium mobilization. Upon the Wnts binding, the fz receptor directly interacts with the heterotrimeric G-protein, and then leads to PLC activation. Subsequently, the plasma membrane component PIP2 is cleaved into DAG and IP$_3$, which binds its receptor IP$_3$R on ER, and thereby ensuring the calcium release.

6. Dishevelled (dsh)

Dishevelled (Dsh) is a core component of both canonical Wnt pathway and planar cell polarity (PCP) pathway. It was originally identified in *Drosophila* according to the phenotype of disorientation in wing hair. Dishevelled also have three homologues (termed Dvl1 - Dvl3), which have been identified in humans and mice.

For the function and structure, Dsh is a cytoplasmic phosphoprotein with multiple

domains. These domains include an N-terminal DIX (Dishevelled, Axin) domain of

80 amino acids, a central PDZ (Postsynaptic density 95, Discs Large, Zonula

occludens-1) domain of about 90 amino acids, and a C-terminal DEP (Dishevelled ,

Egl-10, Pleckstrin) domain of 80 amino acids (Boutros et al., 1999).

The DIX domain in Dsh is similar to the domain in Axin. A single DIX domain

has a compact fold with five β-strands and one α-helix (Schwarz et al., 2007), and this

structure is important to do head-to-tail interaction between two different surfaces of

DIX domain, so that it may promote protein-protein interactions between Dsh and

Axin (Hsu et al., 1999). The PDZ domain in Dsh is a modular protein interaction

domain with two α-helices and six β-sheets to form a peptide-binding cleft (Cheyette

et al., 2002), thus functions as a signal transducer through interacting with Fz directly

(Wong et al., 2003). The C terminal DEP domain consists of three α-helices, two short

β-strands, and one β-hairpin formed by two β-strands (Wong et al., 2000), and its

interact with Daam1 or Rac1 is required for PCP signaling (Veeman et al., 2003).

Furthermore, another two conserved domains, termed basic domain and proline-rich

(PR) domain, which locate preceding and right after the PDZ domain, respectively,

are also implicated to mediate the interaction between Dsh and other members.

7. Multiple Wnt receptors

In alternative Wnt pathways, there are several transmembrane proteins that act as specific receptors for Wnt proteins, including Frizzled, LRP, ROR, and Derailed/RYK.
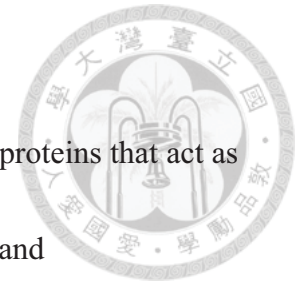
Frizzled (fz) is the major receptor in alternative Wnt pathways. It is a seven-transmembrane receptor, which could interact with Wnts through the extracellular CRD domain itself. In *Drosophila*, there are four fz receptors, including fz, fz2, fz3, and fz4. Among these receptors which could interact with different Wnts specifically, fz and fz2 could bind Wg, Dwnt-2, and DWnt-4; fz3 could bind Wg and Dwnt-2; fz4 could bind DWnt-4 and DWnt-8. In particular, fz and fz2 regulate canonical Wnt pathway (Wg signaling in *Drosophila*) redundantly (Bhat KM 1998) (Bhanot P et al., 1999).

LRPs (arrow/arr in *Drosophila*) are long single-pass transmembrane proteins. They could bind Wnts directly through the extra-cellular domain and form a complex with the Frizzled receptor (Tamai et al., 2000). In addition, the cytoplasmic tail of LRP could be phosphorylated by GSK3 (Zeng et al., 2005) and CK1 (Davidson et al., 2005) kinases, and the phosphorylated domain on LRP would bind to Axin (Tamai et al., 2004) to inhibit the destruction complex, thus required for the canonical Wnt pathway (Wehrli et al., 2000).

RORs are transmembrane tyrosine kinases, they could bind to Wnts by a CRD motif similar to that of the Frizzled (Kani et al., 2004) (Mikels et al., 2006). However, a previous report showed that Wnt5a can inhibit canonical Wnt signaling thorugh binding to ROR2 specifically (Mikels et al., 2006), but the mechanism of this inhibition is unclear.

Derailed proteins are transmembrane tyrosine kinases. They have Wnt binding domain to interact with DWnt5, which could mediate axon guidance in *Drosophila* (Yoshikawa et al., 2003). They also can interact with Dsh (Lu et al., 2004), thus function in Wnt/β-catenin signaling.

8. Other molecules involved in Wnt signaling

GSK3 (shaggy/sgg in *Drosophila*) is a critical regulator in canonical Wnt signaling. It can phosphorylate β-catenin, which is subsequently led to degradation. However, when canonical Wnt signaling is activated, GSK3 would phosphorylate the tail of LRP, and the β-catenin would be released, thereby turn on the downstream signaling. Moreover, GSK3 also plays a multiple non-Wnt related role in other pathways, such as insulin signaling and Hedgehog signaling.

TCF, which is located in the nucleus, also plays a critical regulator in canonical Wnt pathway. It acts as a repressor of canonical Wnt target genes (Riese et al., 1997)

(Bienz 1998) in the absence of the Wnt signals. This repression is mediated by the

TCF-Groucho complex. Otherwise, β-catenin can convert TCF into a transcriptional

activator of the same genes that are repressed by TCF.

9. Hypothesis

There are many molecules involved in large-scale dendrite pruning in *Drosophila*

have been identified, but the mechanism of this developmental event is still elusive.

To further dissect the pruning process, we can either investigate the relationship

between these well-known members, or isolate more novel pruning regulators.

Previous study showed that UPS initiates the dendrite pruning (Kuo et al., 2005),

so that the proteasome activity may play an essential role during early pupal stage. To

address the relationship between UPS and other regulators, we should provide an

available system to detect the dynamics of proteasome activity. According to a report

in *C.elegans*, we can establish a similar photoconvertible reporter of the UPS (Hamer

et al., 2010) in *Drosophila* to know the change of proteasome activity under various

genetic backgrounds, so that we may find the UPS-dependent pruning pathways. Thus,

the first specific aim is to establish a valuable UPS reporter system.

To isolate novel molecules involved in *Drosophila* dendrite pruning, we can do

the genetic screen through recombining candidate alleles with *ppk-Gal4>*

mCD8::GFP, which expresses GFP signals specifically in the class IV da neurons, to examine the neuronal morphology at 16 h APF. Since the remnants of severed dendrites from ddaC neurons were eliminated completely at 16 h APF, the persistence of primary dendrites still attached to the soma (not severed/unsevered/uncut) or present of numerous fragments of dendrite debris (unclean) in candidates would be evidence for its defect in dendrite pruning.

Emerging roles of Wnts include the differentiation of synaptic specializations, microtubule dynamics, architecture of synaptic protein organization, modulation of synaptic efficacy and regulation of gene expression (Speese et al., 2007). In 2009, Hayashi et al. also reported that the Wnt-Ror kinase signaling can regulate neuronal pruning in *C.elegans* (Hayashi et al., 2009). This finding highlighted the regulatory roles of Wnt signaling in neuronal development. Thus, the second specific aim is to investigate the involvement of Wnt pathway. To address this possibility, we used genetic screen to verify several factors of multiple Wnt pathways. In the genetic screen, we examined the phenotypes of two class IV da neurons, the dorsal ddaC neurons and the ventral-lateral v'ada neurons. Because the ddaC neuron initiates its pruning before the v'ada, we will focus on the morphological changes of ddaC in this thesis, whereas the defect of v'ada serves as secondary references for discussion of pruning regulation. We also define that the percentage of uncut phenotype above the

30% in ddaC and the uncut phenotypes above the 50% in v'ada neurons as critical

severing defects, the percentage of uncut phenotype about 5-10%, the unclean

phenotypes above 40% in ddaC, and the uncut phenotypes above 20% in v'ada

neurons as minor pruning defects. The percentage of uncut phenotype lower than 5%,

the unclean phenotypes lower than 40% in ddaC, and the uncut phenotypes lower than

20% in v'ada neurons as little or no pruning defects. Therefore, we can know the

importance of the candidate alleles in each genetic screen for dendrite pruning.
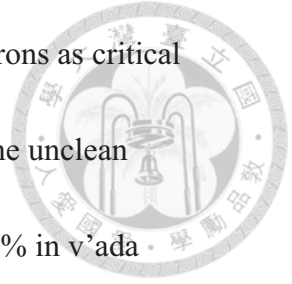
Chapter 2. Materials & Methods

Fly strains

All *Drosophila* strains used in this thesis are listed in Tables. Flies were raised at 25℃ and fed with standard fly food to maintain their growth. For specific expression of UAS-driven transgenes or RNAi in class IV da neurons, *ppk(pickpocket)-Gal4* was used. For observation of neuronal morphology, *ppk-mCD8-GFP* and *ppk-eGFP* were used. In addition, *Ub-dendra2* and *Dendra2* were used as reporters for proteasome activity.

Pupae dissection

First, gently move a pupa out of the tube by forceps, and then adhere the pupa with ventral side down on the slide with double-side tape. Next, use forceps to remove the puparium operculum, expose the head of pupa, then cut the pupa case from anterior to posterior. After that, pull out the pupa gently, transfer it to a new slide, and surround with high vacuum grease (DOW CORNING). Finally, the pupa is immersed with ddH$_2$O, covered with cover slip, and took for confocal imaging.

Confocal imaging

For images of class IV da neurons at 16h APF, pupae were processed by pupae dissection and then imaged by confocal microscope. All images were taken by Nikon D-ECLIPSE 80i, except for the images of Dendra2 conversion (Figure 2A,B), which were acquired from Zeiss LSM700. The former was processed by confocal software (EZ-C1 3.90) and the latter was processed by confocal software (ZEN 2009).

Photoconversion experiment

First, pick up a 3rd instar larva which expressing Ub-Dendra2 or Dendra2 fluorescent proteins, and then directly mount this larva with halocarbon oil on the slide. The orientation of larva is turned exactly with ventral side down, covered by cover slip gently. Next, put this conversion sample onto the heat plate of automatic temperature controller (Warner TC-324B) with the temperature maintained at 25℃, and then take it for confocal processing. Use confocal microscope (Zeiss LSM700) to convert the Dendra2 proteins of ddaC neurons from green to red fluorescence twice with 10min interval, and two methods are applied after the photoconversion step. In Method-1, we image the ddaC neurons of the same larva at four time points (2h, 6h, 10h, and 14h) to trace the fluorescence changes. In Method-2, we convert various

larvae twice, and image the ddaC neurons of each larva at 2h and a final time point (4h, 6h, 8h, 10h, etc).

Conversion data analysis

For conversion data analysis, we process the images of each ddaC neurons by confocal software (ZEN 2009). First, we draw four different lines across the soma to quantify and calculate the average red fluorescence intensity of this neuron, as well as the average red fluorescence intensity of background, at each time point. Then, the net value of red fluorescence intensity can be acquired by subtracting the red fluorescence intensity of background from red fluorescence intensity of background. Finally, the average percentage of red fluorescence intensity at each time point is showed by dividing the red fluorescence intensity at 2h, and thus plots the graph of red fluorescence to represent the dynamics of UPS activity.

Chapter 3. Results

1. The relationship between the dynamics of proteasome activity and *Drosophila* dendrite pruning
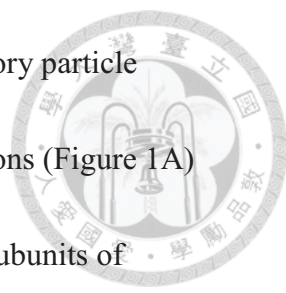
According to previous study of the involvement of UPS (Kuo et al., 2005), it suggested that loss of functions of proteasome subunits might also cause pruning defects, as well as the dynamics of proteasome activity may also change with this proteasome dysfunction. To test this hypothesis, we did knockdown experiments of proteasome subunits to examine the morphological changes of class IV da neurons first, and then used photoconvertible reporter system to detect the changes of proteasome activity to investigate their association.

1.1 Knockdown of proteasome subunits in class IV da neurons caused pruning defects

To do loss-of-function experiments of proteasome, we used several *Drosophila* RNAi strains to examine the phenotypes of class IV da neurons at 16h APF. Because of the complexity of proteasome, we roughly divided these subunits of proteasome into two groups, including Rpn ttt(regulatory particle subcomplex) subunits and DTS (core particle subcomplex) subunits. The first group consisted of six *Rpn RNAi* lines

(*Rpn1, Rpn2, Rpn6, Rpn10, Rpn14#1,* and *Rpn14#2*). These regulatory particle

subunits showed almost minor uncut phenotypes in both ddaC neurons (Figure 1A)

and v'ada neurons (Figure 1B). These data suggested that the Rpn subunits of

proteasome have merely small effect on pruning process. The second group consisted

of three *DTS RNAi* lines (*DTS5#1, DTS5#2,* and *DTS7*). Two strains of *DTS RNAi*

(*DTS5#1* and *DTS7*) showed minor uncut phenotypes in ddaC neurons (Figure 1C)

and v'ada neurons (Figure 1D) just as the six *Rpn RNAi* lines above. However, the

DTS5 RNAi#2 exhibited critical defects (Figure 1F, F') compared to *wild type (WT)*,

and had high levels of uncut phenotypes both in ddaC (Figre 1C) and v'ada neurons

(Figure 1D). To exclude the possibility that this sharply significant difference was

caused by other genetic side effects but not the knockdown of *DTS5*, we examined the

no-Gal4-driver control group of *DTS5 RNAi#2*, and then found it had no statistical

significances (Figure 1C, D) as well as shared similar phenotypes (Figure 1G, G')

compared to *WT* both in ddaC and v'ada neurons. These data suggested that the *DTS5*

RNAi#2 has high efficiency on its knockdown experiment, and the core subunit DTS5

may affect dendrite pruning because it result in proteasome dysfunction.

1.2 The proteasome activities of Ub-Dendra2 and Dendra2 control in WT ddaC neurons during the larval stage
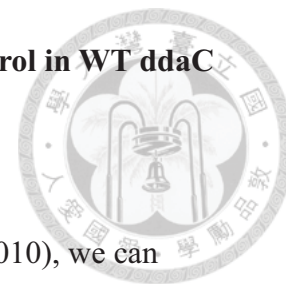
According to the previous report in *C.elegans* (Hamer et al., 2010), we can develop a photoconversion-based fluorescence method to image and quantify proteasome activity in ddaC neurons of *Drosophila*. Dendra2 is a fluorescence protein, which can be irreversibly photoconverted from a green to a red fluorescent state by excitation of the chromophore with 405 nm light (Figure 2A,B). Thus, we can use this characteristic to quantify the photoconverted fluorescent signals to report the degradation of these reporter proteins, and further to reflect the proteasome activity. Here, we generated *Drosophila* strains that can express the ubiquitin-fused Dendra2 mutant form that would target this fluorescent protein for proteasome-dependent degradation pathway, and provided two methods for the establishment of this reporter system in larval stage. In Method-1, we used the same larva for photoconversion experiments. After the second photoconversion, this larva would be imaged at four time points (2h, 6h, 10h, and 14h) with 4h interval (Figure 2C). In Method-2 , we provided several larvae for photoconversion experiments, each larva would be imaged at two time points (2h and final time point), and finally combined the data of each larva to show the whole pattern of fluorescent changes with 2h interval (Figure 2C). Here, we performed Ub-Dendra2 photoconversion experiments through Method-1

(Figure 2D) and Method-2 (Figure 2F), and found a decreasing pattern of fluorescence intensity. On the other hand, the photoconversion experiments of Dendra2 control through both Method-1 (Figure 2E) and Method-2 (Figure 2G) showed that a stable pattern of converted fluorescent signals. These data suggested that a clear degradation of Ub-Dendra2 could be observed compared to Dendra2 control, and this consequence performed similarly by either Method-1 or Method-2.
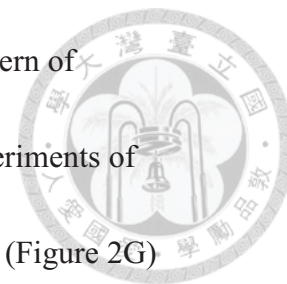
1.3 The proteasome activity of Ub-Dendra2 under knockdown of *DTS5* and *UAS-lacZ* control backgrounds during the larval stage

To further verify the changes of proteasome activity when the function of proteasome was lost, as well as the relationship between the pruning process and the dynamics of proteasome activity, we examined the proteasome activity of *DTS5 RNAi#2*, which caused critical pruning defects. By Method-2, we observed that the decreasing pattern of Ub-Dendra2 under *WT* genetic background (Figure 2F) would be rescued under the *DTS5 RNAi* genetic background (Figure 2H). In addition, the *UAS-lacZ* control, which were be performed to exclude the possible side effects of Gal4 driver, showed a similar pattern (Figure 2I) with Ub-Dendra2 under *WT* genetic background. Totally, we established an available reporter system that could reflect the dynamics of UPS activity during *Drosophila* larval stage.
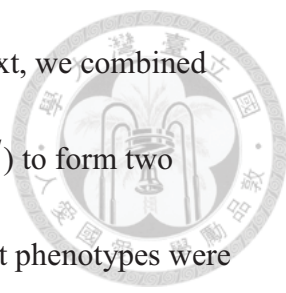
2. Loss-of-function analysis of *dishevelled* in class IV da neurons
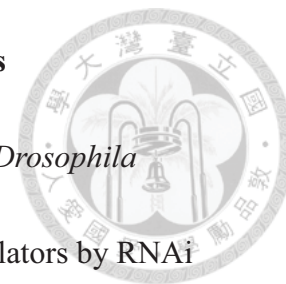
As mentioned previously, because few molecules involved in *Drosophila* dendrite pruning have been identified, we should isolate novel regulators by RNAi screen. According to our hypothesis, Wnt pathway might play an essential role in the dendrite pruning process, so we would use this knockdown approach to examine the neuronal morphology of Wnt-related RNAi lines, such as dsh protein. Thus, two strains of *dsh RNAi* were performed, and a critical dendrite severing defect was observed both in ddaC (Figure 3B, C) and v'ada neurons (Figure 3B', C'). Quantitative analysis also showed high percentages of dendrite severing defects in both ddaC (Figure 3D) and v'ada neurons (Figure 3E), especially the *dsh RNAi#1*. These results indicated that dsh protein may be a potential regulator of *Drosophila* dendrite pruning.

2.1 The *dsh* mutants showed minor dendrite severing defects
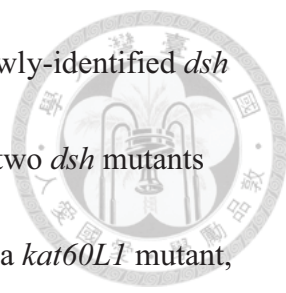
By RNAi screen, we identified *dsh* as a novel factor that might affect dendrite pruning. Due to the possible off-target effect of *dsh RNAi*, we should examine *dsh* mutants to confirm the regulatory role of *dsh*. First, we checked the neuronal phenotypes of two *dsh* heterozygous mutant: $dsh^3/+$ and $dsh^6/+$, and a *dsh* hemizygous hypomorph: dsh^1/Y. However, these *dsh* mutants showed little severing

defect both in ddaC (Figure 4A) and v'ada neurons (Figure 4B). Next, we combined

each heterozygous mutant (dsh^3 and dsh^6) with the hypomorph (dsh^1) to form two

transheterozygous mutants: dsh^3/dsh^1 and dsh^6/dsh^1, but little uncut phenotypes were

observed both in ddaC (Figure 4C) and v'ada neurons (Figure 4D). These inconsistent

results with the *dsh RNAi* might be caused by the minor deficiencies on heterozygotes

and hypomorphs. To address this possibility, we generated two strong *dsh* hemizygous

mutants: dsh^6/Y and dsh^{G0267}/Y (dsh^3/Y was dead before the 3rd instar larval stage).

Compared to *WT* (Figure 5A, A'), both hemizygous mutants exhibited a primary

dendrite attached to soma in ddaC (Figure 5B, C) and v'ada neurons (Figure 5B', C').

Quantitative analysis of these mutants showed minor uncut phenotypes in ddaC

(Figure 5E) and v'ada neurons (Figure 5F). In addition, dsh^6/Y also showed high

percentages (about 40%) of unclean phenotypes (Figure 5D, D') in class IV da

neurons. Together, studies of these *dsh* mutants suggested a minor role to regulate

Drosophila dendrite severing.

2.2 The genetic interaction between *dsh* and three identified regulators (*Ik2*,

kat-60L1, and *Spn-F*) in class IV da neurons
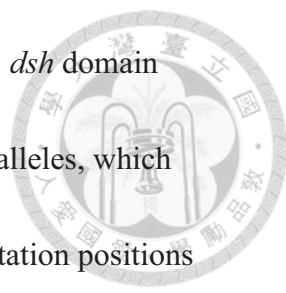
Previous studies in our lab showed that *katanin p60-like 1 (kat60L1)*, *Ik2,* and

Spindle-F (Spn-F) are crucial regulators in the *Drosophila* dendrite pruning, so we

wondered whether these molecules have genetic interaction with newly-identified *dsh*

to regulate the pruning process. To address this idea, we performed two *dsh* mutants

(dsh^3 and dsh^6) recombined with two *Ik2* mutants ($Ik2^1$ and $Ik2^{alice}$), a *kat60L1* mutant,

and a *Spn-F* mutant ($Spn-F^2$) to investigate their genetic interaction. The

transheterozygous experiments showed that neither the dsh^3 nor the dsh^6 could

enhance dendrite severing defects with two *Ik2* mutants in both ddaC (Figure 6A, C)

and v'ada neurons (Figure 6B, D). It also showed that almost clean phenotypes (no

pruning defects) of two transheterozygotes, $dsh^3/+; kat60L1/+$ and $dsh^6/+; kat60L1/+$

(Figure 6E), as well as $dsh^3/+; Spn-F^2/+$ and $dsh^6/+; Spn-F^2/+$ (Figure 6G), in ddaC

neurons. Similarly, no enhanced dendrite severing defects of *dsh/+; kat60L1/+*

transheterozygotes ($dsh^3/+; kat60L1/+$ and $dsh^6/+; kat60L1/+$) (Figure 6F) and *dsh/+;*

Spn-F/+ transheterozygotes ($dsh^3/ +; Spn-F^2/+$ and $dsh^6/+; Spn-F^2/+$) (Figure 6H) in

v'ada neurons. Taken together, these studies indicated that there were no genetic

interactions between *dsh* and three factors to regulate dendrite pruning.

2.3 Mutational analysis of *dsh* with distinct mutated domains showed various

morphological changes of dendrite pruning defects

To further determine which pathway the *dsh* is involved to regulate dendrite

pruning, we did domain-specific mutational analysis of *dsh* to examine the

corresponding obvious uncut phenotypes. According to the previous *dsh* domain

analysis in *Drosophila* (Penton et al., 2002), there were several *dsh* alleles, which

could be roughly divided into to three groups on the basis of the mutation positions

within *dsh*. The Group I alleles (*dsh^{A3}*, *dsh^{A21}*, and *dsh^{1}*, a hypomorph allele showed

previously) encode mutations within the DEP domain of *dsh*. The DEP domain can

interact with Daam1 or Rac1, and is required for PCP signaling (Veeman et al., 2003).

These PCP-signaling-dependent *dsh* mutnats showed little severing defects in ddaC

(Figure 7A) and v'ada neurons (Figure 7B). Thus, this experiment excluded the role

of PCP pathway in dendrite pruning process. The Group II alleles (*UAS-dsh$^{8-16}$* and

UAS-dsh$^{8-65}$) encode missense mutations within the DIX domain of *dsh*. The DIX

domain can interact with Axin, and is required for Wg signaling. However, there were

no statistically significanct differences of dendrite severing compared to *WT* observed

in the two DIX-domain-mutated *dsh* alleles in ddaC (Figure 7C) and minor severing

defects in v'ada neurons (Figure 7D). Surprisingly, the Group III alleles (*UAS-dsh$^{8-12}$*

and *UAS-dsh$^{8-79}$*), which encode missense mutations within the PR domain of *dsh*,

exhibited obvious dendrite severing defects in ddaC (Figure 7E) and high percentages

of dendrite severing in v'ada neurons (Figure 7F). Compared to *WT* (Figure 7G, G'),

expression of PR-domain-mutated *dsh* caused some primary dendrites to remain

attached to soma both in ddaC (Figure 7H, I) and v'ada neurons (Figure 7H', I').

These data indicated that *dsh* might regulate dendrite pruning through the PR-domain-dependent canonical Wnt pathway.
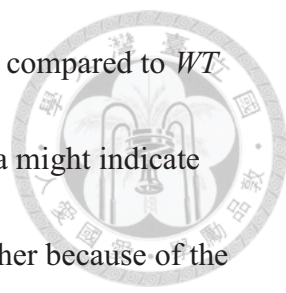
3. Loss-of-function analysis of multiple Wnt receptors in class IV da neurons

Given that loss of function of *dsh* could cause pruning defect, we wondered which Wnt receptor upstream of *dsh* is involved. Here, we examined the multiple Wnt receptor mutant strains, including *Drosophila fz* to *fz4*, *Ror*, *derailed*, and also a co-receptor, *arrow*, to further explore the involvement of Wnt pathway in dendrite pruning.

3.1 Loss-of-function analysis of two redundant Wnt receptors, *fz* and *fz2*, showed minor dendrite severing defects

Based on the mutational analysis of *dsh* with distinct mutated domains, it was suggested that *dsh* may influence pruning through PR-domain-dependent Wg signaling. In support of this notion, we speculated that the upstream receptors might be *fz* and *fz2*, which were reported to regulate Wg signaling redundantly (Bhat KM 1998) (Bhanot P et al., 1999). To address this hypothesis, we first examined the *fz* and *fz2* mutants, including two heterozygous mutants, $fz^{1}/+$ and $fz2^{CPTI003490}/+$, as well as a homozygous mutant $fz2^{NP3337}/fz2^{NP3337}$. However, quantitative analysis of dendrite

severing defects showed that no statistically significanct differences compared to *WT* in both ddaC (Figure 8A) and v'ada neurons (Figure 8B). These data might indicate that the defects of these mutants might be complemented by each other because of the redundant roles of *fz* and *fz2*. Next, we generated three transheterozygates: (1) fz^1/+, $fz2^{CPTI003490}$/+, (2) fz^1/+, $fz2^{NP3337}$/+, and (3) $fz2^{CPTI003490}$/$fz2^{NP3337}$ and found no enhancement of severing defects within these transheterozygous mutants either in ddaC neurons (Figure 8A) or v'ada neurons (Figure 8B); otherwise, these transheterozygous mutants showed critical unclean phenotypes (Figure 8D, E, F) compared to WT (Figure 8C), and the percentages of the unclean phenotypes within fz^1/+, $fz2^{CPTI003490}$/+ and fz^1/+, $fz2^{NP3337}$/+ were also enhanced compared to fz^1/+ and $fz2^{CPTI003490}$/+ in both ddaC (Figure 8A') and v'ada neurons (Figure 8B'). These findings raised the possibility that *fz* and *fz2* should work redundantly to turn on Wg signaling but had minor effects on dendrite pruning.

Owing to the minor defects within the *fz* and *fz2* mutants, we wondered whether knockdown of overall *fz* and *fz2* may result in obvious pruning defects. We examined five *fz RNAi* strains and five *fz2 RNAi* strains, and quantify the percentages of uncut phenotypes in class IV da neurons. Quantitative analysis showed that little severing defects were observed in ddaC neurons of either *fz RNAi* (Figure 9A) or *fz2 RNAi* strains (Figure 9C), but half of v'ada neurons (Figure 9B, D) exhibited severing

defects within some *fz RNAi* and *fz2 RNAi* strains. These results, consistent with the

mutational analysis of *fz* and *fz2*, suggested that minor roles of these two Wnt

receptors in dendrite pruning process. Furthermore, we also did double knockdown of

both *fz* and *fz2*, but surprisingly, quantitative analysis of dendrite severing defects

showed no enhancement in ddaC neurons (Figure 9E) and even largely reduced

percentages in v'ada neurons (Figure 9F). It may suggest that the amounts of RNAi

driver Gal4 were shared by both *fz RNAi* and *fz2 RNAi*, and thus result in the low

efficiencies of these knockdown experiments.

3.2 Other receptors involved in multiple Wnt pathways

Because of the minor effects of both *fz* and *fz2*, it raised a possibility that maybe

other Wnt receptors play major roles to regulate dendrite pruning. In *Drosophila*,

other *fz* receptors, *fz3* and *fz4*, as well as the two transmembrane tyrosine kinases, *ror*

and *drl*, can bind Wnt ligands to regulate Wnt signaling. Here, we generated two

hemizygous mutants and four homozygous mutants, including $fz3^{CB\text{-}5443\text{-}3}/Y$,

$fz4^{GS7412}/Y$, $ror^{LL01120}/ror^{LL01120}$, ror^{GS107}/ror^{GS107}, $drl^{LL05382}/drl^{LL05382}$ and

drl^{PGAL8}/drl^{PGAL8}, to check the pruning phenotypes themselves. However,

quantification of severing defect in both ddaC and v'ada neurons of these multiple

Wnt receptor mutants had no statistical differences compared to *WT* (Figure 10A, B).

These data excluded the involvement of these four receptors in dendrite pruning.
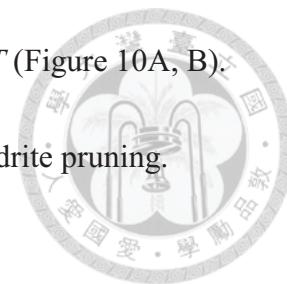
3.3 Mutational analysis of Wg co-receptor *arrow* showed some dendrite pruning defects

LRP (*arr* in *Drosophila*) is a co-receptor, which form a complex with the

Frizzled receptor to regulate Wg signaling. On the basis of the previous data, the

essential PR domain of *dsh* and the minor effects of *fz/+, fz2/+* loss of function, it

suggested that the Wg signaling may be involved in dendrite pruning, and furthermore,

highlighted the regulatory role of Wg signaling specific co-recrptor *arr*. To verify if

arr can affect dendrite pruning, we examined the neuronal morphology of two

heterozygous mutants: $arr^{EY04553}$/+ and $arr^{MI03803}$/+ (these strains are homozygous

lethal). Compared to *WT* (Figure 11A,A'), we observed $arr^{EY04553}$/+ and $arr^{MI03803}$/+

exhibited some uncut phenotypes in ddaC (Figure 11B,C) and v'ada neurons (Figure

11B', C') with the percentages about 10% in ddaC (Figure 11D) and about 40-60% in

v'ada neurons (Figure 11E). These data indicate that *arr* might be essential to regulate

dendrite pruning, and is consistent with the mutational experiments of *dsh* and Wg

receptors. To further investigate if the *arr* and *dsh* have genetic interaction through

Wg signaling, we generated some *dsh/+; arr/+* transheterozygous mutants: dsh^3/+;

$arr^{EY04553}$/+, dsh^6/+; $arr^{EY04553}$/+, dsh^3/+; $arr^{MI03803}$/+, and dsh^6/+; $arr^{MI03803}$/+.

However, transheterozygous experiments showed that the percentages of pruning

defects in both ddaC (Figure F,H) and v'ada (Figure G,I) were significantly reduced

when compared to *arr/+* controls. These results might suggest that *dsh* negatively

regulates *arr* through other unclear mechanisms.
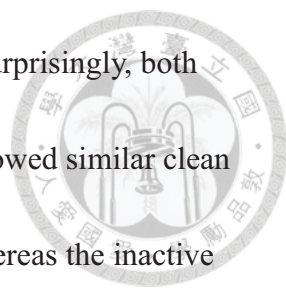
4. Loss-of-function analysis of other Wnt members downstream of *dsh* in class IV da neurons

Given that the canonical Wnt pathway might play a role to regulate dendrite

pruning, we wondered which Wnt member downstream of *dsh* was involved, and thus

can further confirm the Wg signaling regulation in *Drosophila* dendrite pruning. Here,

we would investigate the involvement of a negative regulator *sgg*, and a nuclear

transcriptional activator *TCF* in dendrite pruning.

4.1 Expression of various mutant forms of sgg caused critical severing defects

In the canonical Wnt pathway, *GSK3 (sgg)* is a key negative regulator, which

comprises the destruction complex to inhibit β-catenin. To verify the influence of *sgg*

in dendrite pruning, we examined three transgenic lines expressing *sgg* proteins

bearing mutations: *UAS-sgg.S9A/+* (constitutively active form), *UAS-sgg.A81T* /+

(inactive form), and *UAS-sgg.KK83-84RK/+* (kinase dead form). Surprisingly, both

ddaC and v'ada neurons of constitutively active *UAS-sgg.S9A/+* showed similar clean

phenotypes (Figure 12B, B') compared to *WT* (Figure 12A, A'), whereas the inactive

UAS-sgg.A81T/+ and kinase dead *UAS-sgg.KK83-84RK/+* exhibited numbers of

primary dendrites still attached to the soma in both ddaC (Figure 12C, D) and v'ada

neurons (Figure 12C' ,D'). Quantitative analysis of severing defects in both two class

IV da neurons also showed that a *WT*-like low percentage of *UAS-sgg.S9A/+*, but

more than 90% severing defects within the *UAS-sgg.A81T/+* and

UAS-sgg.KK83-84RK/+ (Figure 12E, F). These results were in opposition to our

hypothesis that the dendrite pruning is regulated by activated canonical Wnt pathway.

4.2 Expression of N-terminal-deletion TCF mutant form caused critical severing defects

TCF, a transcriptional repressor of Wnt target genes, will be converted into a

transcriptional activator in the presence of the Wnt signals. The N-terminal of *TCF*

provides a binding site for β-catenin, thus a dominant negative effect will occur when

we deleted the N-terminal of *TCF*. To confirm the importance of canonical Wnts, we

expressed a dominant negative *UAS-pan.dTCFΔN/+*. Compared to *WT* (Figure13 A,

A'), strong severing defects were observed within this *UAS-pan.dTCFΔN/+* either in

ddaC (Figure 13B) or v'ada neurons (Figure 13B'). These class IV da neurons

exhibited nearly no severed dendritic branches. All of primary dendrites were still

attached to the soma, just as the neurons in the larval stage. Quantitative analysis also

represented around 90% of uncut phenotypes both in the ddaC (Figure 13C) and v'ada

neurons (Figure 13D). As a consequence, we further confirmed the role of canonical

Wnt pathway to mediate *Drosophila* dendrite pruning, and found a critical regulator

TCF.
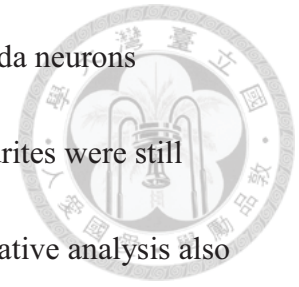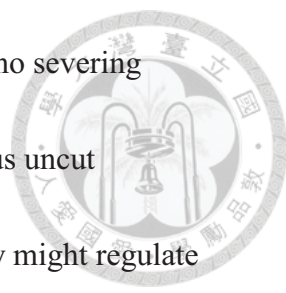
Chapter 4. Discussion

In our studies, we did knockdown experiments of several proteasome subunits first, and found a critical severing defect within the *DTS5 RNAi#2* strain which caused the core particle subunit DTS5 knockdown. Then, we developed a photoconvertible reporter system through *Drosophila* strains expressing the ubiquitin-fused Dendra2 which targeted this fluorescent protein for UPS-dependent protein degradation. The following photoconversion experiments during larval stage showed that a clear degradation of Ub-Dendra2 compared to Dendra2 control through both two methods of different time courses. Finally, we used this photoconvertible reporter system under *DTS5 RNAi#2* genetic background, which caused severe pruning defects, to verify the change of proteasome activity. The photoconversion experiments showed that the clear degradation of Ub-Dnedra2 would be restored with proteasome dysfunction, and thus demonstrated the availability of this fluorescent reporter.

To isolate novel pruning regulators in *Drosophila*, we used genetic screen and found critical severing defects within the *dsh RNAi*. However, several *dsh* mutants showed only minor or even no severing defects. To further determine the regulatory role of *dsh* in dendrite pruning, we did mutational analysis with various domain-specific *dsh* mutants. Surprisingly, either the PCP-dependent DEP domain

mutants or the Wg-dependent DIX domain mutants showed almost no severing

defects, but the Wg-dependent PR domain mutants exhibited obvious uncut

phenotypes. These results suggested that the canonical Wnt pathway might regulate

dendrite pruning. In support of this notion, we examined several Wnt receptor mutants,

including *fz* to *fz4*, *ror*, *drl*, as well as a co-receptor *arr*. In these mutational

experiments, *fz* and *fz2* worked redundantly and showed minor effects on dendrite

pruning, whereas the co-receptor *arr* exhibited some severing defects of class IV da

neurons. Consistent with the mutational analysis of *dsh*, these data suggested the

canonical Wnt pathway could affect pruning process. Finally, to ensure the Wg

signaling can regulate dendrite pruning, we examined the N terminal deletion mutant

form *TCF*, a transcriptional activator of Wnt target genes, and found critical severing

defects in class IV da neurons at 16h APF. Taken together, these results indicated the

canonical Wnt can mediate *Drosophila* dendrite pruning.

1. The application of photoconvertible reporter system of the UPS

Based on previous study in *C.elegans*, we expressed a fluorescent protein

Ub-Dendra2 in *Drosophila* to establish an available UPS reporter system. In contrast

to other methods, use this reporter system can separate the protein degradation from

protein synthesis. It can be used to quantify the UPS-dependent protein degradation

through a ubiquitin-fusion manner. For the application of this available reporter in

Drosophila, we can express Ub-Dendra2 in the different cell types by tissue-specific

Gal4 to investigate the different functions of UPS activity in selected cell types. We

can quantify the UPS activity to calculate the degradation rate in particular conditions.

Importantly, we can also express Ub-dendra2 in either larval or pupal stage to explore

some physiological events which are influenced by the dynamics of proteasome

activity.

2. The mutational analysis of *Dishevelled*
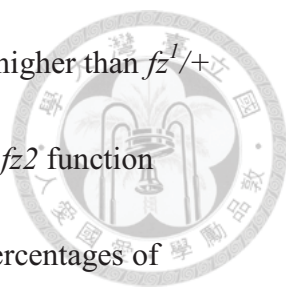
Based on the RNAi screen, we found that *dsh* knockdown can result in critical

dendrite severing defect, and then suggested that *dsh* plays an essential role in

Drosophila dendrite pruning. In support of this notion, we used several *dsh* mutants,

such as dsh^6 and dsh^{G0267}, to examine the neuronal phenotypes, but the percentages of

unsevered neurons were low. Because *dsh* is required for both Wg and PCP signaling

and is very important in the fly development processes, the mutants with critical

defective neurons might be lethal before 16h APF and thus we cannot observe them.

To further dissect the role of *dsh* in dendrite pruning, we examined the dominant

negative mutants with point mutation on specific domain of *dsh*, and found that the

mutation on PR domain of *dsh* caused dendrite severing defects, whereas mutation on

other domains of *dsh* showed no significances. These results raise the importance of

dsh PR domain which also involved in Wg signaling. The interaction between *dsh* and

other proteins through this domain might be a possible mechanism to regulate

dendrite pruning, so PR-domain-interacting factors will be good candidates for next

genetic screens.

3. The roles of two redundant Wnt receptors, *Frizzled* and *Frizzled2*, as well as the co-receptor *arrow*
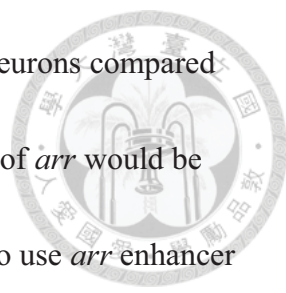
To demonstrate the hypothesis that Wg signaling is required for dendrite pruning,

we examined the mutants of *fz* and *fz2*, which were reported as redundant Wg

receptors. However, we found little pruning defects in these mutants. There are some

reasons to explain this phenomenon. First, the effects of these mutants are not obvious

because the *fz* mutant fz^1 and *fz2* mutant $fz^{CPTI003490}$ are both homozygous lethal, we

can just observe the minor effects of heterozygous $fz^1/+$ and $fz2^{CPTI003490}/+$. Second,

the two *fz2* mutants were generated by transposable element insertion and the

insertion sites are located at intron, so the influence of the *fz2* mutation is small. Third,

the *fz* and *fz2* are redundant, so one of them can complement the other' function.

Because of these possibilities, we further did transheterozygous and knockdown

experiments. We found that transheterozygotes $fz^1/+$, $fz2^{CPTI003490}/+$ showed low

percentage of uncut phenotype but nearly half unclean phenotypes, higher than fz^1/+ and $fz2^{CPTI003490}$ /+. This result is consistent with the fact that fz and $fz2$ function redundantly. Moreover, single knockdown of fz or $fz2$ caused low percentages of uncut phenotypes in dorsal ddaC neurons just as in mutants, but higher percentages of uncut phenotypes in ventral v'ada neurons than mutants. However, double knockdown of both fz and $fz2$ showed reduced pruning defects in both ddaC and v'ada neurons. These data suggested that lower the amounts of Wg receptors can slightly affect pruning process, but the efficiencies of double knockdown is bad owing to the fact that the Gal4 drivers would be shared. Taken together, fz and $fz2$ might redundantly regulate dendrite pruning. To further dissect their regulatory roles in class IV da neurons, we will use several enhancer trap lines (Table 3) to verify their expression patterns to ensure the presence of these Wg receptors in class IV da neurons.

In addition, we also examined the neuronal phenotypes of the arr heterozygous mutants (arr^{EY0455}/+ and $arr^{MI03803}$/+), which exhibited about 10% uncut phenotypes in ddaC and 40-60% uncut phenotypes in v'ada neurons, higher than fz and $fz2$. Because arr is required for Wg signaling, this data can support our hypothesis that the canonical Wnt pathway can regulate *Drosophila* dendrite pruning. However, when we did transheterozygous experiments to address the genetic interaction between arr and

dsh, we observed reduced pruning defects in both ddaC and v'ada neurons compared to *arr* heterozygotes. These data indicated that perhaps the function of *arr* would be inhibited by *dsh* in some elusive mechanisms. Similarly, we will also use *arr* enhancer trap lines to confirm its expression in class IV da neurons, and do some genetic interaction between *arr* and other members of Wg signaling, such as Wg receptors, *fz* and *fz2*, or some negative regulators, *sgg*, and *Axin*.

4. Possible mechanisms for Wnt signaling to regulate dendrite pruning

Totally, either in the *dsh* mutants, or in the Wg receptor (*fz*, *fz2* and *arr*) mutants, there are some phenomena that could be discussed. We found that these mutants exhibited delayed developmental progress. The pupal cases of these mutants were too soft, and the development of legs was abortive at 16h APF, despite the head invasion stage is accomplished. This finding indicated that the mutation of these upstream regulators delay the fly development, especially the dendrite pruning. We can verify this possibility by examining the neuronal phenotypes at the earlier 12h APF.

For the downstream effectors of Wg signaling, surprisingly, we found that the expression of mutant form *sgg*, a negative regulator of Wg, can cause critical dendrite severing defects. Due to the multiple non-Wnt related roles in other pathways (such as insulin signaling and Hedgehog signaling) of *sgg*, this data suggested that there are

sgg-associated critical pathways can regulate dendrite pruning. To demonstrate this

possibility, we can use genetic screen to examine the key regulators of the pathways

which *sgg* is involved. In addition, the genetic interaction experiments between *sgg*

and other Wg members can further verify the role of *sgg* in the canonical Wnt

pathway.

The N-terminal deletion form of *TCF*, a transcription activator of Wg target

genes, also caused high percentages of uncut phenotypes in class IV da neurons. This

result strongly demonstrates that Wg signaling can regulate dendrite pruning. To

confirm the possibility of this regulation, we can examine the neuronal phenotypes of

other *TCF* dominant negative mutants. Moreover, we can also screen the Wnt target

genes to isolate some novel regulators.

5. Crosstalk between protein degradation and Wnt pathway in dendrite pruning

In this thesis, we first developed a photoconvertible reporter system to detect

proteasome activity, and then found the involvement of Wg signaling in *Drosophila*

dendrite pruning. The Wg signaling members now become good candidates of the

UPS reporter system. It is interesting to ask a question if there is any crosstalk

between UPS-dependent protein degradation pathway and Wg signaling during

dendrite pruning process. To address this possibility, we will examine the proteasome

activity under *dsh RNAi* genetic backgrounds to investigate if the dysfunction of Wg

can interrupt the proteasome' function. Furthermore, we also can detect Wnt target

gene expression under *DTS5 RNAi* genetic background to explore if the UPS can

affect Wg signaling. Together, we will find the association of protein degradation and

Wnt pathway.
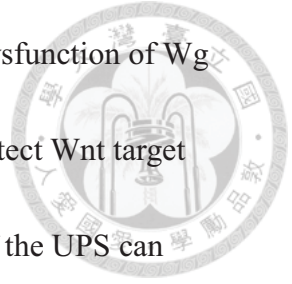
Chapter 5. References

Bhanot P, Fish M, Jemison JA, Nusse R, Nathans J, Cadigan KM. (1999) Frizzled and

Dfrizzled-2 function as redundant receptors for Wingless during Drosophila

embryonic development. Development 126(18):4175-86.

Bhat KM. (1998) frizzled and frizzled 2 play a partially redundant role in wingless

signaling and have similar requirements to wingless in neurogenesis. Cell

95(7):1027-36.

Bienz M. (1998) TCF: transcriptional activator or repressor? Curr Opin Cell Biol.

10(3):366-72.

Boutros M, Mlodzik M. (1999) Dishevelled: at the crossroads of divergent

intracellular signaling pathways. Mech Dev. 83(1-2):27-37.

Cheyette BN, Waxman JS, Miller JR, Takemaru K, Sheldahl LC, Khlebtsova N, Fox

EP, Earnest T, Moon RT. (2002) Dapper, a Dishevelled-associated antagonist of

beta-catenin and JNK signaling, is required for notochord formation. Dev Cell

2(4):449-61.

Davidson G1, Wu W, Shen J, Bilic J, Fenger U, Stannek P, Glinka A, Niehrs C. (2005)

Casein kinase 1 gamma couples Wnt receptor activation to cytoplasmic signal

transduction. Nature 438(7069):867-72.

Finley D. (2009) Recognition and processing of ubiquitin-protein conjugates by the

proteasome. Annu Rev Biochem. 78:477-513.

Grueber WB, Jan LY, Jan YN. (2002) Tiling of the Drosophila epidermis by

multidendritic sensory neurons. Development 129(12):2867-78.

Hamer G, Matilainen O, Holmberg CI. (2010) A photoconvertible reporter of the

ubiquitin-proteasome system in vivo. Nat Methods 7(6):473-8.

Hanna J, Finley D. (2007) A proteasome for all occasions. FEBS Lett.

581(15):2854-61.

Hayashi Y, Hirotsu T, Iwata R, Kage-Nakadai E, Kunitomo H, Ishihara T, Iino Y,

Kubo T. (2009) A trophic role for Wnt-Ror kinase signaling during developmental

pruning in Caenorhabditis elegans. Nat Neurosci 12(8):981-7.

Hsu W, Zeng L, Costantini F. (1999) Identification of a domain of Axin that binds to

the serine/threonine protein phosphatase 2A and a self-binding domain. J Biol

Chem. 274(6):3439-45.

Hwang RY, Zhong L, Xu Y, Johnson T, Zhang F, Deisseroth K, Tracey WD. (2007)

Nociceptive neurons protect Drosophila larvae from parasitoid wasps. Curr Biol.

17(24):2105-16.

Johnson ES1, Bartel B, Seufert W, Varshavsky A. (1992) Ubiquitin as a degradation

signal. EMBO J. 11(2):497-505.

Kanamori T, Kanai MI, Dairyo Y, Yasunaga K, Morikawa RK, Emoto K. (2013)
Compartmentalized calcium transients trigger dendrite pruning in Drosophila
sensory neurons. Science 340(6139):1475-8.
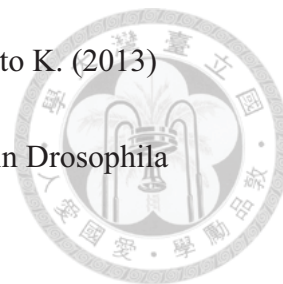
Kani S, Oishi I, Yamamoto H, Yoda A, Suzuki H, Nomachi A, Iozumi K, Nishita M,
Kikuchi A, Takumi T, Minami Y. (2004) The receptor tyrosine kinase Ror2
associates with and is activated by casein kinase Iepsilon. J Biol Chem.
279(48):50102-9.

Kirilly D, Gu Y, Huang Y, Wu Z, Bashirullah A, Low BC, Kolodkin AL, Wang H, Yu
F. (2009) A genetic pathway composed of Sox14 and Mical governs severing of
dendrites during pruning. Nat Neurosci. 12(12):1497-505.

Kuo CT, Jan LY, Jan YN. (2005) Dendrite-specific remodeling of Drosophila sensory
neurons requires matrix metalloproteases, ubiquitin-proteasome, and ecdysone
signaling. Proc Natl Acad Sci U S A. 102(42):15230-5.

Kuo CT, Zhu S, Younger S, Jan LY, Jan YN. (2006) Identification of E2/E3
ubiquitinating enzymes and caspase activity regulating Drosophila sensory neuron
dendrite pruning. Neuron 51(3):283-90.

Lee HH, Jan LY, Jan YN. (2009) Drosophila IKK-related kinase Ik2 and Katanin
p60-like 1 regulate dendrite pruning of sensory neuron during metamorphosis.
Proc Natl Acad Sci U S A. 106(15):6363-8.

Lee T, Lee A, Luo L. (1999) Development of the Drosophila mushroom bodies: sequential generation of three distinct types of neurons from a neuroblast. Development 126(18):4065-76.

Loncle N, Williams DW. (2012) An interaction screen identifies headcase as a regulator of large-scale pruning. J Neurosci. 32(48):17086-96.

Lu W, Yamamoto V, Ortega B, Baltimore D. (2004) Mammalian Ryk is a Wnt coreceptor required for stimulation of neurite outgrowth. Cell 119(1):97-108.

Marin EC, Watts RJ, Tanaka NK, Ito K, Luo L. (2005) Developmentally programmed remodeling of the Drosophila olfactory circuit. Development 132(4):725-37.

Mikels AJ1, Nusse R. (2006) Purified Wnt5a protein activates or inhibits beta-catenin-TCF signaling depending on receptor context. PLoS Biol. 4(4):e115.

Penton A, Wodarz A, Nusse R. (2002) A mutational analysis of dishevelled in Drosophila defines novel domains in the dishevelled protein as well as novel suppressing alleles of axin. Genetics 161(2):747-62.

Riese J, Yu X, Munnerlyn A, Eresh S, Hsu SC, Grosschedl R, Bienz M. (1997) LEF-1, a nuclear factor coordinating signaling inputs from wingless and decapentaplegic. Cell 88(6):777-87.

Rumpf S, Lee SB, Jan LY, Jan YN. (2011) Neuronal remodeling and apoptosis require

VCP-dependent degradation of the apoptosis inhibitor DIAP1. Development

138(6):1153-60.

Schwarz-Romond T, Fiedler M, Shibata N, Butler PJ, Kikuchi A, Higuchi Y, Bienz M.

(2007) The DIX domain of Dishevelled confers Wnt signaling by dynamic

polymerization. Nat Struct Mol Biol. 14(6):484-92.

Speese SD, Budnik V. (2007) Wnts: up-and-coming at the synapse. Trends Neurosci.

30(6):268-75.

Tamai K, Semenov M, Kato Y, Spokony R, Liu C, Katsuyama Y, Hess F,

Saint-Jeannet JP, He X. (2000) LDL-receptor-related proteins in Wnt signal

transduction. Nature 407(6803):530-5.

Tamai K, Zeng X, Liu C, Zhang X, Harada Y, Chang Z, He X. (2004) A mechanism

for Wnt coreceptor activation. Mol Cell 13(1):149-56.

Veeman MT, Axelrod JD, Moon RT. (2003) A second canon. Functions and

mechanisms of beta-catenin-independent Wnt signaling. Dev Cell. 5(3):367-77.

Wehrli M, Dougan ST, Caldwell K, O'Keefe L, Schwartz S, Vaizel-Ohayon D,

Schejter E, Tomlinson A, DiNardo S. (2000) arrow encodes an

LDL-receptor-related protein essential for Wingless signalling. Nature

407(6803):527-30.

Williams DW, Kondo S, Krzyzanowska A, Hiromi Y, Truman JW. (2006) Local

caspase activity directs engulfment of dendrites during pruning. Nat Neurosci.

9(10):1234-6.

Williams DW, Truman JW. (2005) Cellular mechanisms of dendrite pruning in

Drosophila: insights from in vivo time-lapse of remodeling dendritic arborizing

sensory neurons. Development 132(16):3631-42.

Wong HC, Bourdelas A, Krauss A, Lee HJ, Shao Y, Wu D, Mlodzik M, Shi DL,

Zheng J. (2003) Direct binding of the PDZ domain of Dishevelled to a conserved

internal sequence in the C-terminal region of Frizzled. Mol Cell 12(5):1251-60.

Wong HC, Mao J, Nguyen JT, Srinivas S, Zhang W, Liu B, Li L, Wu D, Zheng J.

(2000) Structural basis of the recognition of the dishevelled DEP domain in the

Wnt signaling pathway. Nat Struct Biol. 7(12):1178-84.

Wong JJ, Li S, Lim EK, Wang Y, Wang C, Zhang H, Kirilly D, Wu C, Liou YC, Wang

H, Yu F. (2013) A Cullin1-based SCF E3 ubiquitin ligase targets the

InR/PI3K/TOR pathway to regulate neuronal pruning. PLoS Biol.

11(9):e1001657.

Xiang Y, Yuan Q, Vogt N, Looger LL, Jan LY, Jan YN. (2010)

Light-avoidance-mediating photoreceptors tile the Drosophila larval body wall.

Nature 468(7326):921-6.

Yoshikawa S, McKinnon RD, Kokel M, Thomas JB. (2003) Wnt-mediated axon

guidance via the Drosophila Derailed receptor. Nature 422(6932):583-8.

Zeng X, Tamai K, Doble B, Li S, Huang H, Habas R, Okamura H, Woodgett J, He X.

(2005) A dual-kinase mechanism for Wnt co-receptor phosphorylation and

activation. Nature 438(7069):873-7.
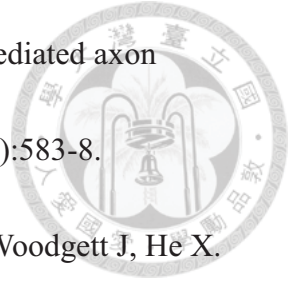
Tables

Table 1. List of fly mutant stocks

dsh lines	statement	source
dsh^{A3}	DEP domain point mutation. Amino acid replacement: R413H.	Cheng-Ting Chien
dsh^{A21}	DEP domain point mutation. Amino acid replacement: C472R.	Cheng-Ting Chien
w; UAS-dsh$^{8-12}$/Tb	PR domain point mutation. Amino acid replacement: P358L.	Cheng-Ting Chien
w; +/CyO; UAS-dsh$^{8-79}$	PR domain point mutation. Amino acid replacement: D360V.	Cheng-Ting Chien
y, w, dsh^3, f^{36a}/FM7a	Deletion of the open reading frame between nucleotides 496 and 1040, resulting in a frameshift after amino acid residue 94.	Cheng-Ting Chien
w^1, dsh^1	DEP domain point mutation. Amino acid replacement: K417M.	Kyoto
dsh^6/FM7a	Mutagen: ethyl nitrosourea. Mutant phenotype is similar to that shown by wg mutants.	Kyoto
w^{67c23}, P{lacW}dsh^{G0267}/FM7c	P-element insertion. Insertion site: 5'-UTR.	Bloomington
w^{118}; P{UAS-dsh$^{8-65}$.myc}3-8	DIX domain point mutation. Amino acid replacement: F40S.	Bloomington
w^{118}; P{UAS-dsh$^{8-16}$.myc}3-8	DIX domain point mutation. Amino acid replacement: G64V.	Bloomington

arr lines	statement	source
$y^1 w^*$; $Mi\{MIC\}arr^{MI03803}$/SM6a	Transposable element insertion. Insertion site: intron near the 3'-UTR.	Bloomington
$y^1 w^{67c23}$; $P\{EPgy2\}arr^{EY04453}$/CyO	P-element insertion. Insertion site: 3'-UTR.	Bloomington

fz lines	statement	source
fz^1/TM1	Spontaneous mutant. Bristle polarity phenotype.	Kyoto

fz2 lines	statement	source
w^{1118}; $PBac\{768.FSVS-0\}$ $fz2^{CPTI003490}$/TM3, Sb	piggyBac insertion. Insertion site: intron near the coding region.	Kyoto
w^*; $P\{GawB\}fz2^{NP3337}$	P-element insertion. Insertion site: intron in some transcripts.	Kyoto

fz3 lines	statement	source
$P\{RS3\}fz3^{CB-5443-3}$, w^{1118}	P-element insertion. Insertion site: near the TSS.	Kyoto

fz4 lines	statement	source
y^1, w^{67c23}, $P\{GSV2\}fz4^{GS7412}$/Bi nsinscy	P-element insertion. Insertion site: 3'-UTR. Insertion oriented to drive expression in the sense direction starting upstream of the coding region.	Kyoto

ror lines	statement	source
$y^* w^*$; $ror^{LL01120}$, cn^1, bw^1/CyO, S^*, bw^1	piggyBac insertion. Insertion site: intron.	Kyoto
y^1, w^{67c23}; ror^{GS8107}/SM1	P-element insertion. Insertion site: 5'-UTR near the TTS.	Kyoto

drl lines	statement	source
$y^* w^*$; $drl^{LL05382}$, cn^1, bw^1/CyO, S^*, bw^1	piggyBac insertion. Insertion site: upstream of the TTS.	Kyoto
w^{1118}; $P\{GawB\}drl^{PGAL8}$	P-element insertion. Insertion site: 5'-UTR near the TTS.	Kyoto

sgg lines	statement	source
w^{1118}; P{UAS-sgg.KK83-84RK}6	Amino acid replacement: K83R and K84K. Expression of the mutated sgg protein (a near kinase dead form).	Hsiu-Hsiang Lee
w^{1118}; P{UAS-sgg.A81T}MB30	Amino acid replacement: A81T. Expression of an inactive form of the sgg gene product.	Hsiu-Hsiang Lee
w^{1118}; P{UAS-sgg.S9A}MB14	Amino acid replacement: S9A. Expression of the sgg SGG10 mutant cDNA. The sgg protein produced is constitutively active.	Hsiu-Hsiang Lee

TCF lines	statement	source
Sp/CyO;ΔN-TCF/TM6B	Lacks the N-terminal β-catenin interaction domain; acts as a dominant negative.	Hsiu-Hsiang Lee

Ik2 lines	source
w; ik2^1, FRT40A/CyO, hs-hid, w$^+$	Hsiu-Hsiang Lee
w; ik2^{alice}, FRT40A/CyO, hs-hid, w$^+$	Hsiu-Hsiang Lee

Spn-F lines	source
SpnF^2, ppk-GFP, e/TM6B, ubi-GFP	Hsiu-Hsiang Lee

kat-60L1 lines	source
kat-60L1, ppk-eGFP/TM6B, Tb	Hsiu-Hsiang Lee

Dendra2 lines	source
ppk-Gal4-Ub-D-8-4-2-2-2/CyO, weep; +/TM6B	Hsiu-Hsiang Lee
ppk-Gal4-den10-2/CyO, weep	Hsiu-Hsiang Lee
ppk-Gal4/CyO, weep; D-CL1-5-1-3/TM6B	Hsiu-Hsiang Lee

Table 2. List of fly RNAi stocks

(I) Nig-Fly

genotype	stock ID
Rpn1 RNAi	7762R-4
Rpn2 RNAi	11888R-1
Rpn6 RNAi	10149R-3
Rpn10 RNAi:	7619R-4
Rpn14 RNAi#1	6789R-1
Rpn14 RNAi#2	6789R-3
DTS7 RNAi	3329R-1
DTS5 RNAi#1	4097R-1
DTS5 RNAi#2	4097R-2
dsh RNAi#1	18361R-2
dsh RNAi#2	18361R-3
fz RNAi#1	17697R-1
fz RNAi#2	17697R-2
fz2 RNAi#1	9739R-1
fz2 RNAi#2	9739R-2

(II) Bloomington

genotype	stock ID
fz RNAi#3	31036
fz RNAi#4	31311
fz RNAi#5	34321
fz2 RNAi#3	31312
fz2 RNAi#4	27568
fz2 RNAi#5	31390
futsch RNAi	40834
tau RNAi#1	40875
tau RNAi#2	28891

Table 3. List of enhancer trap lines

fz lines	source
w^{1118}; $Mi\{ET1\}fz^{MB07478}$	Bloomington
$y^*\ w^*$; $P\{GawB\}fz^{NP5457}$ / TM6, $P\{UAS\text{-}lacZ.UW23\text{-}1\}UW23\text{-}1$	Kyoto
w^*; $P\{GawB\}fz^{NP5624}$	Kyoto
w^*; $P\{GawB\}fz^{NP5629}$ / TM3, $Sb^1\ Ser^1$	Kyoto
w^*; $P\{GawB\}fz^{NP7514}$ / TM6, $P\{UAS\text{-}lacZ.UW23\text{-}1\}UW23\text{-}1$	Kyoto

fz2 lines	source
$y^1\ w^{67c23}$; $Mi\{ET1\}fz2^{MB01455}$	Bloomington
w^*; $P\{GawB\}fz2^{NP3337}$	Kyoto

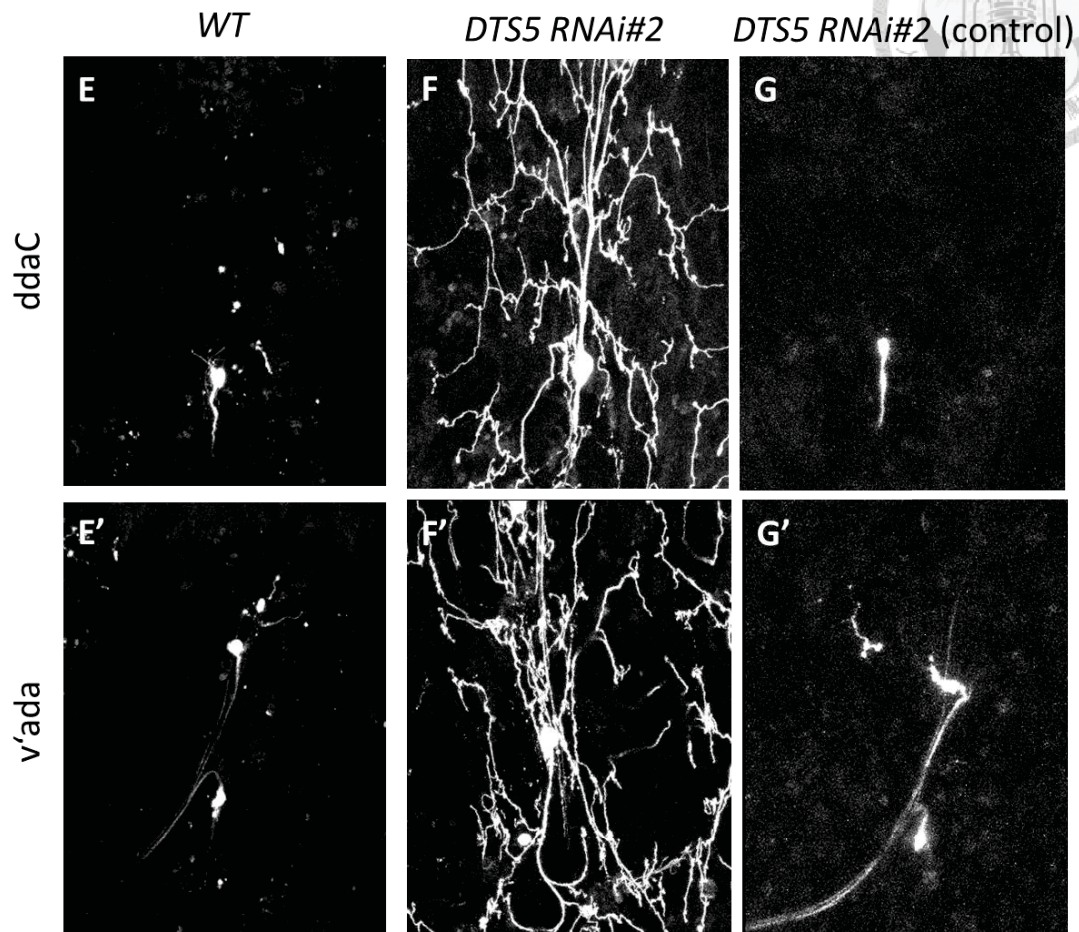| *arr* lines	source
$y^1\ w^{67c23}$; $P\{lacW\}arr^{k08131}$/CyO	Bloomington

Figure 1
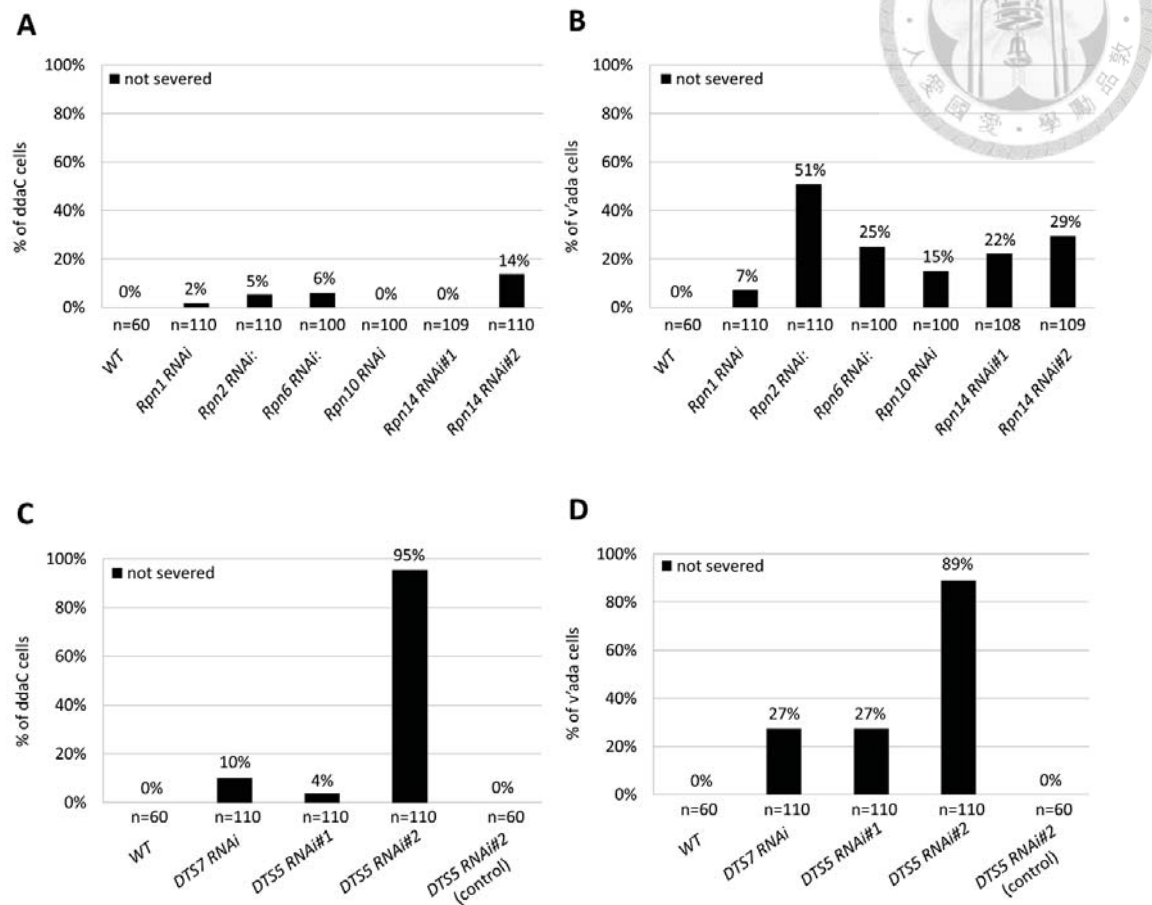
Figure 1. Knockdown of proteasome subunits in class IV da neurons caused

dendrite pruning defect

ddaC and v'ada neurons were visualized by expressing *UAS-mCDGFP* driven by

ppk-Gal4 at 16h APF. (A,B) Quantitative analysis of dendrite severing defects in

ddaC neurons (A) and v'ada neurons (B) under the proteasome-subunit *Rpn RNAi*

backgrounds. (C,D) Quantitative analysis of dendrite severing defects in ddaC

neurons (C) and v'ada neurons (D) under the proteasome-subunit *DTS RNAi*

backgrounds.

Figure 1 (continued)

Figure 1. Knockdown of proteasome subunits in class IV da neurons caused dendrite pruning defect

ddaC neurons (E) and v'ada neurons (E') of *WT*. (F,G) Dendrite severing defects were observed in (F) ddaC neurons and (F') v'ada neurons of *DTS5 RNAi#2*, whereas ddaC neurons (G) and v'ada neurons (G') serve as no Gal4 driver control of *DTS5 RNAi#2*. The percentages of ddaC/v'ada cells represent the number of unsevered neurons dividing the number of total ddaC/v'ada cells, respectively. The number of ddaC/v'ada neurons in each group is indicated under the bar.
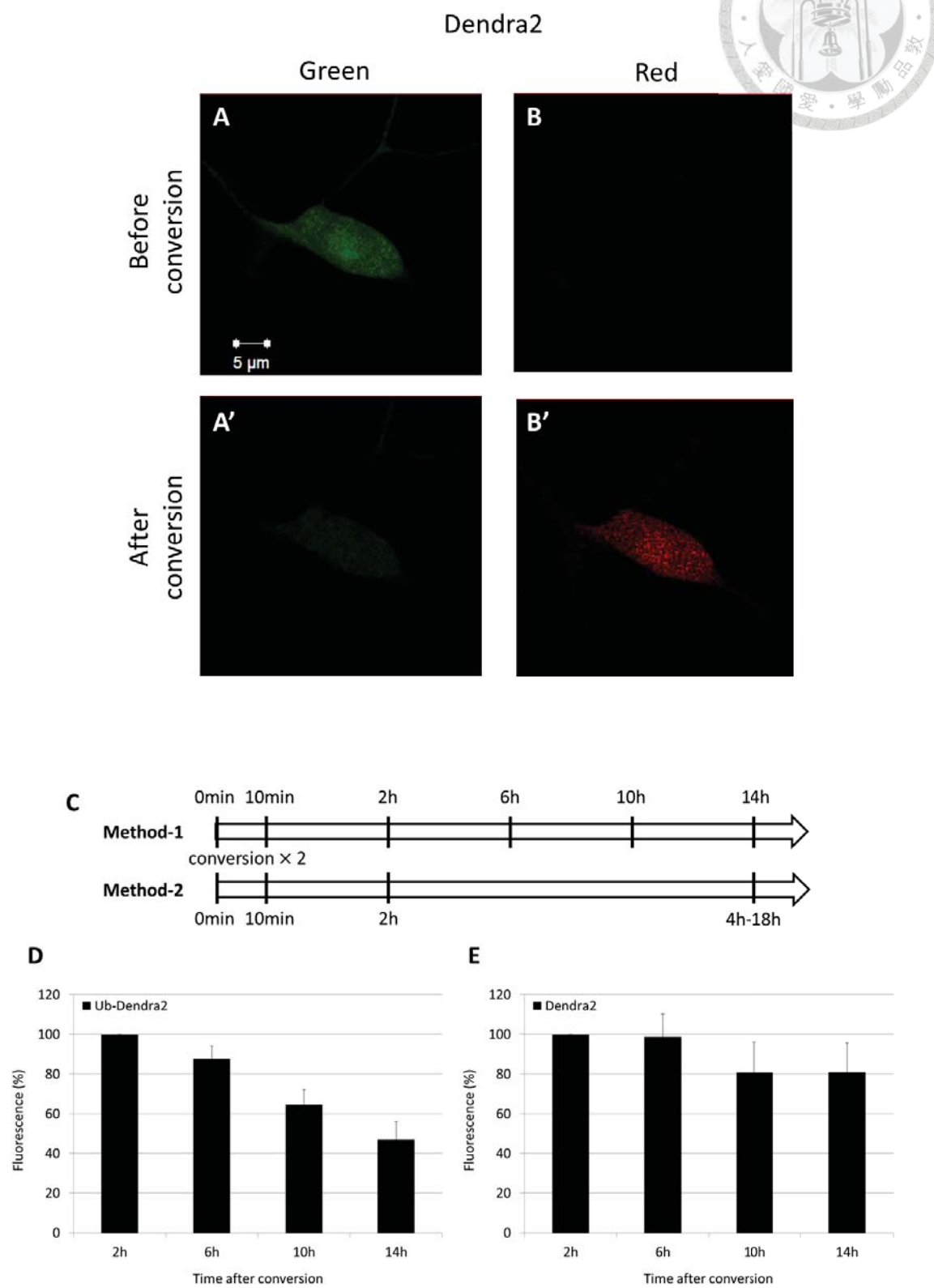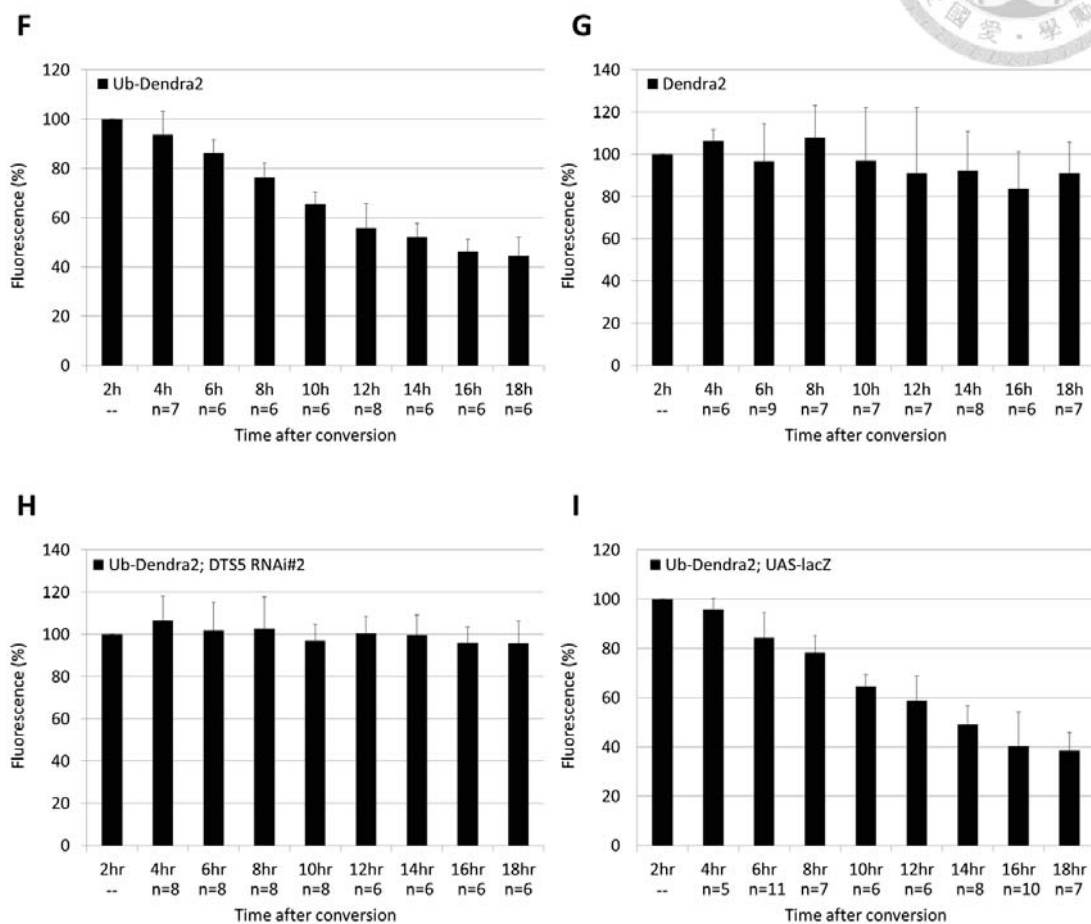
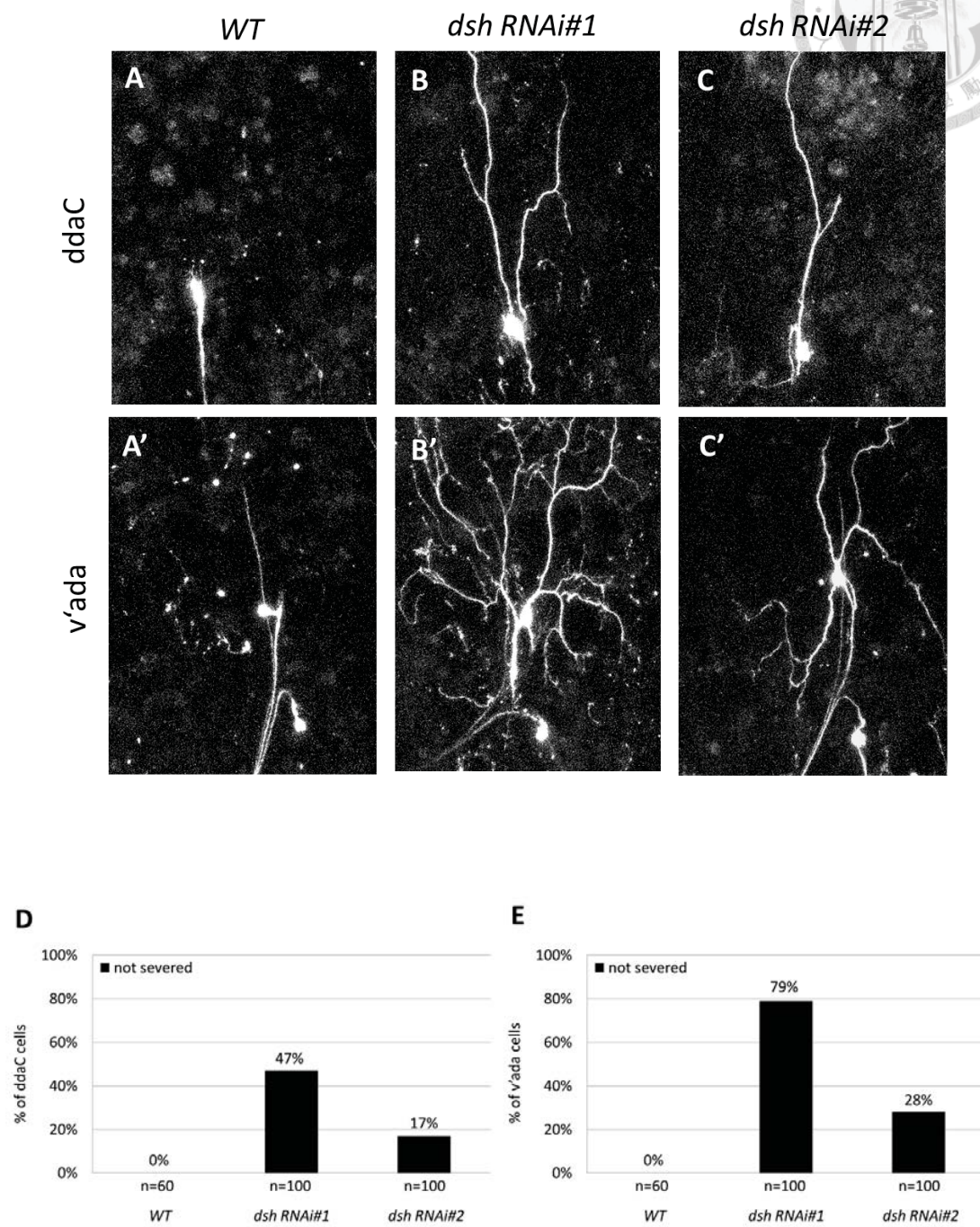# Figure 2

Figure 2 (continued)

Figure 2 (continued)

Figure 2. Proteasome activities of Ub-Dendra2 in class IV da neurons during the larval stage

(A,B) Representative fluorescence micrographs of *Drosophila* larva expressing Dendra2 in ddaC neurons, imaged before and after photoconversion. (C) Diagraph showed the time courses of two methods for photoconversion experiments. (D,E) The graphs showed average percentages of red fluorescence intensity relative to that at 2h to quantify the degradation of Ub-Dendra2 (D, n=6)) and Dendra2 (E, n=11) by Method-1. (F,G) The graphs showed average percentages of red fluorescence intensity relative to that at 2h to quantify the degradation of Ub-Dendra2 (F) and Dnedra2 (G) by Method-2. The number of ddaC neurons in each time point groups is indicated under the bar. (H,I) Degradation of Ub-Dendra2 by Method-2 under the genetic background of knockdown of the proteasome subunit *DTS5* (H) and the *UAS-lacZ* control (I).
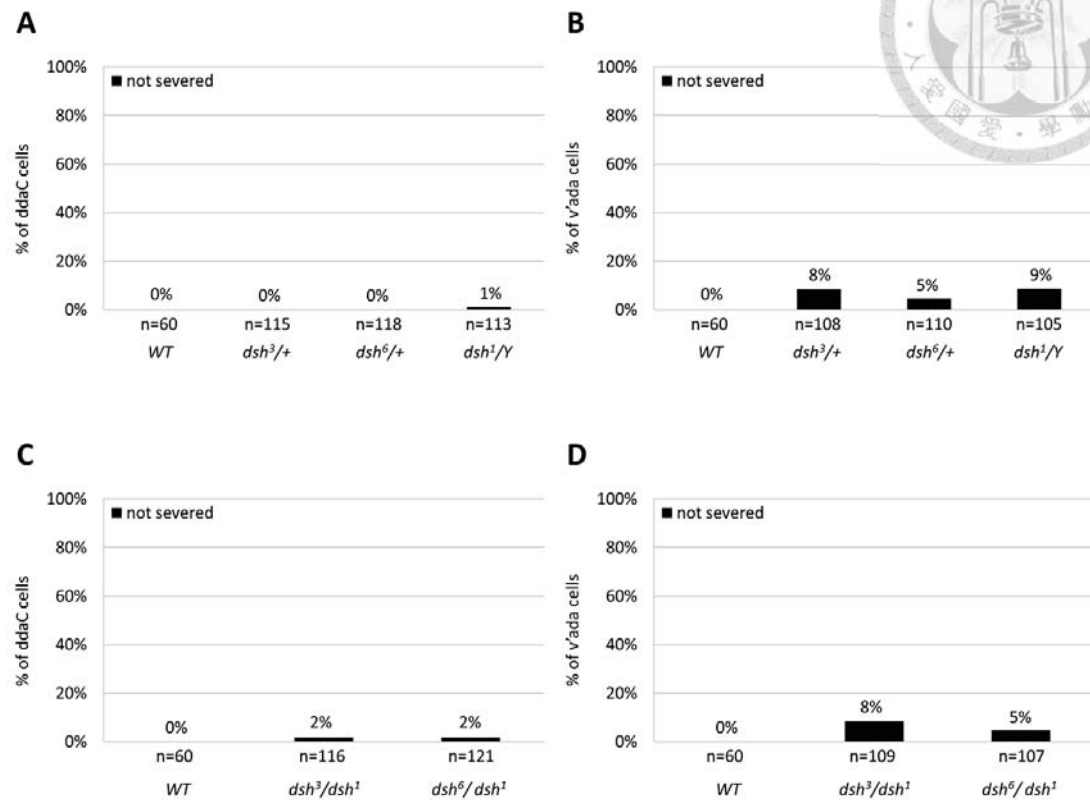
Figure 3

Figure 3 (continued)

Figure 3. Knockdown of *dsh* caused critical dendrite pruning defect

ddaC and v'ada neurons were visualized by expressing *UAS-mCDGFP* driven by

ppk-Gal4 at 16h APF. (A) ddaC neurons and (A') v'ada neurons of *WT*. (B,C) Dendrite

severing defects were observed in (B) ddaC neurons and (B') v'ada neurons of *dsh*

RNAi#1 and in (C) ddaC neurons and (C') v'ada neurons of *dsh RNAi#2*. (D,E)

Quantitative analysis of dendrite severing defects in ddaC neurons (D) and v'ada

neurons (E) under the *dsh RNAi* backgrounds. The percentages of ddaC/v'ada cells

represent the number of unsevered neurons dividing the number of total ddaC/v'ada

cells, respectively. The number of ddaC/v'ada neurons in each groups is indicated

under the bar.

Figure 4

Figure 4. No severing defect were observed in *dsh* mutants

ddaC and v'ada neurons were visualized by expressing *UAS-mCDGFP* driven by

ppk-Gal4 at 16h APF. (A,B) Quantitative analysis of dendrite severing defects in

ddaC neurons (A) and v'ada neurons (B) under the *dsh/+* heterozygous mutant

backgrounds. (C,D) Quantitative analysis of dendrite severing defects in ddaC

neurons (C) and v'ada neurons (D) under the *dsh* transheterozygous mutant

backgrounds. The percentages of ddaC/v'ada cells represent the number of unsevered

neurons dividing the number of total ddaC/v'ada cells, respectively. The number of

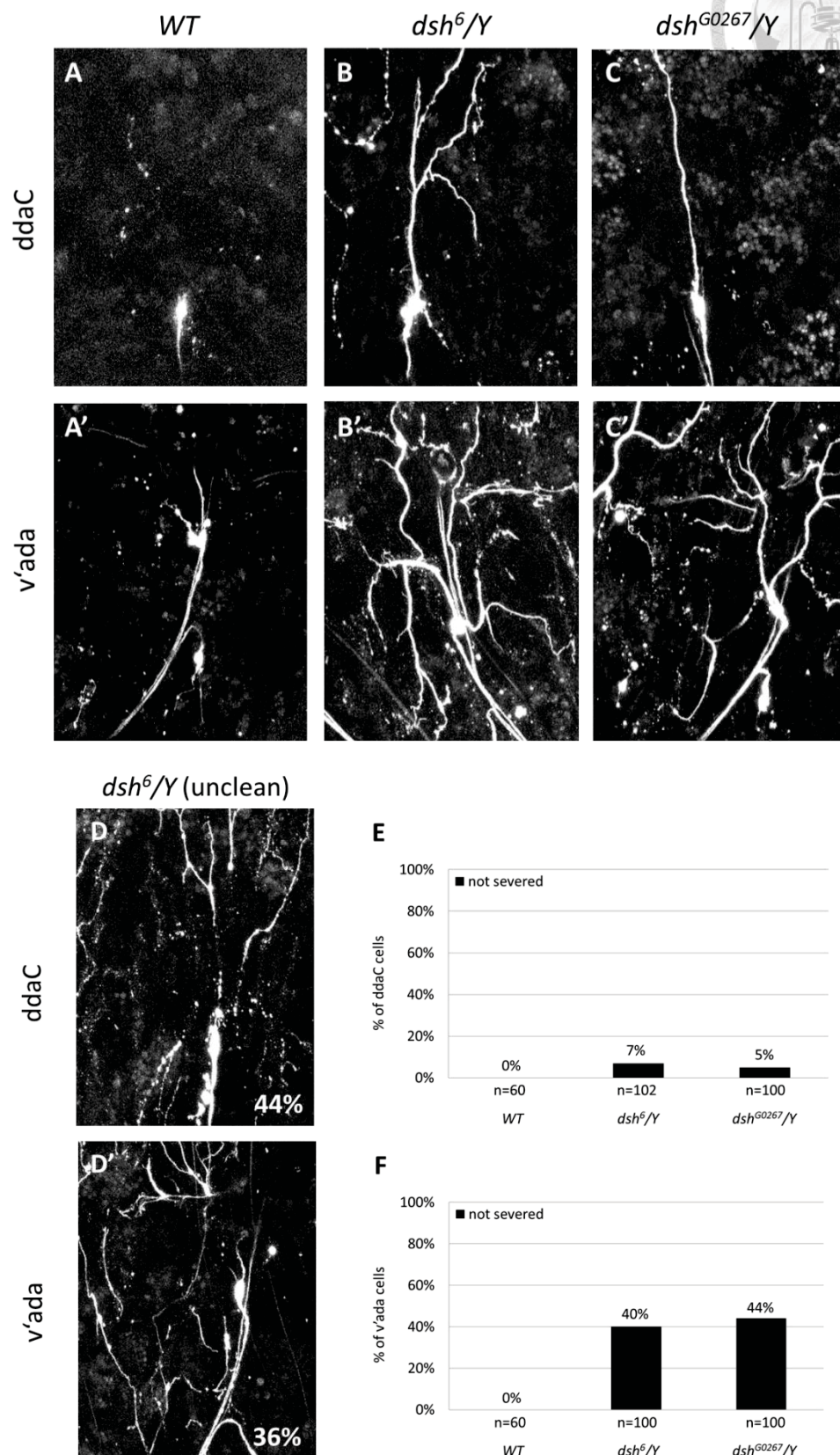ddaC/v'ada neurons in each group is indicated under the bar.

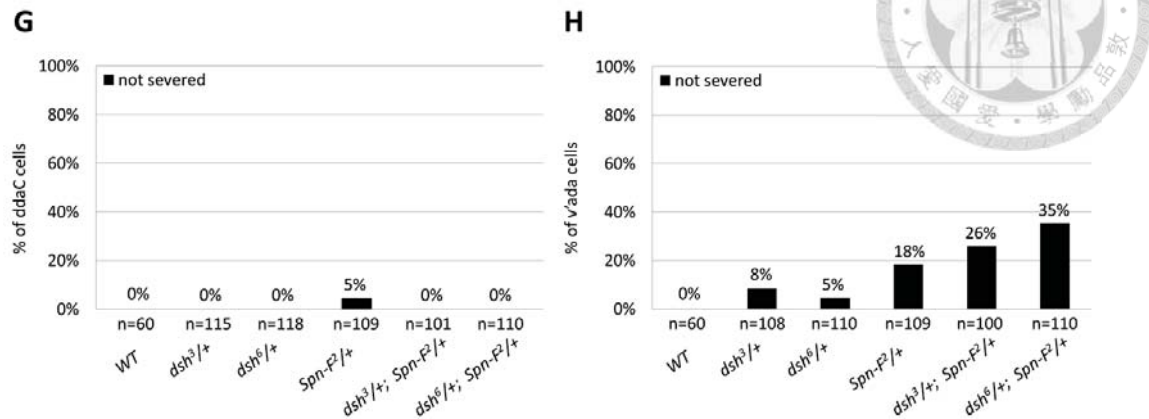# Figure 5

Figure 5 (continued)

Figure 5. *Dsh* hemizygous mutants caused minor severing defect

ddaC and v'ada neurons were visualized by expressing *UAS-mCDGFP* driven by

ppk-Gal4 at 16h APF. (A) ddaC neurons and (A') v'ada neurons of *WT*. (B,C) Dendrite

severing defects were observed in (B) ddaC neurons and (B') v'ada neurons of dsh^6/Y

hemizygous mutant and in (C) ddaC neurons and (C') v'ada neurons of dsh^{G0267}/Y

hemizygous mutant. (D) ddaC neurons and (D') v'ada neurons showed severe unclean

phenotype of dsh^6/Y hemizygous mutant. (E,F) Quantitative analysis of dendrite

severing defects in ddaC neurons (E) and v'ada neurons (F) under the *dsh/Y*

hemizygous mutant backgrounds. The percentages of ddaC/v'ada cells represent the

number of unsevered neurons dividing the number of total ddaC/v'ada cells,

respectively. The number of ddaC/v'ada neurons in each group is indicated under the

bar.

Figure 6
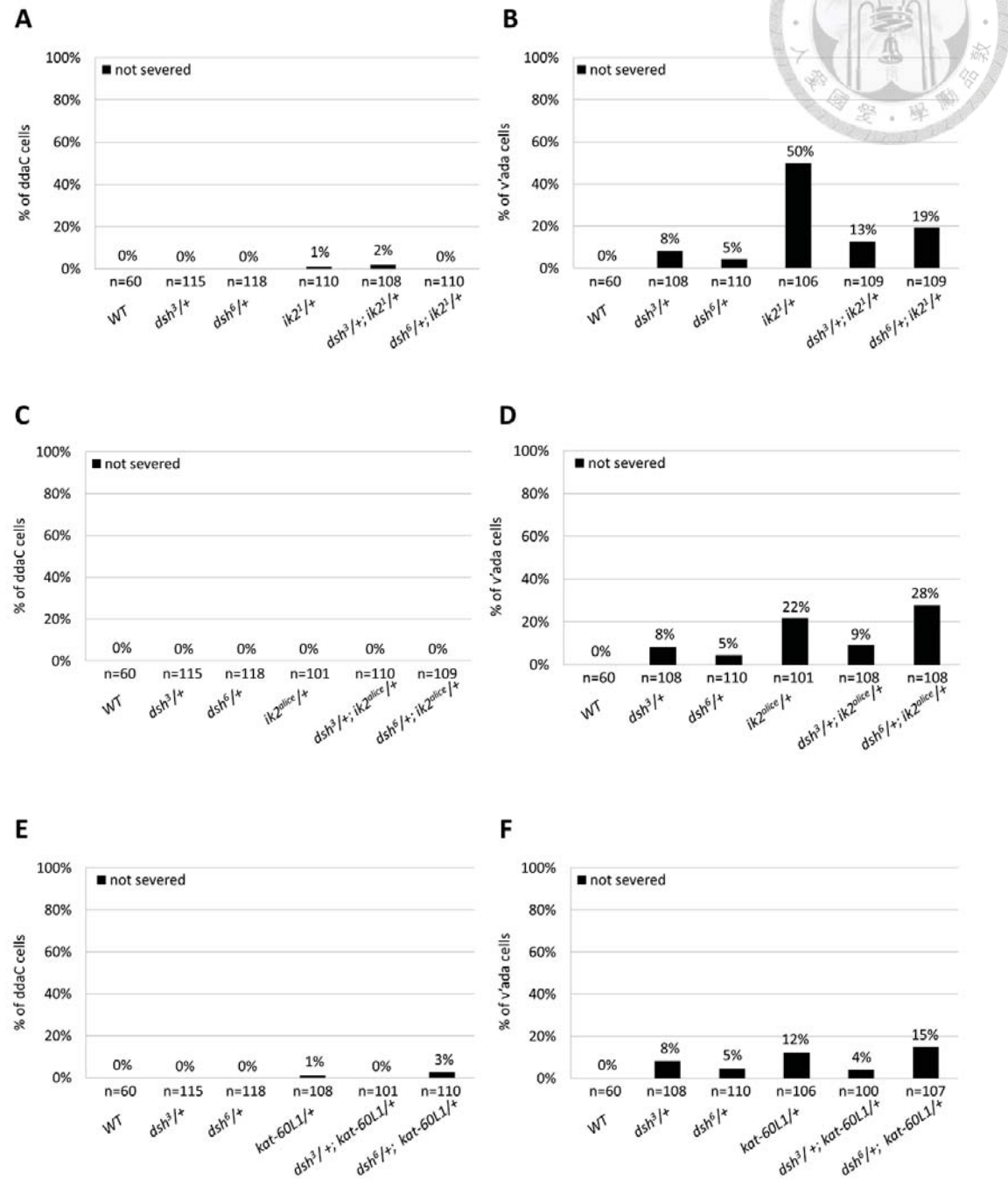
Figure 6 (continued)

Figure 6. The genetic interaction between *dsh* and three identified regulators (*Ik2*, *kat-60L1*, and *Spn-F*) in class IV da neurons

ddaC and v'ada neurons were visualized by expressing *UAS-mCDGFP* driven by

ppk-Gal4 at 16h APF. (A-D) Quantitative analysis of dendrite severing defects in

ddaC neurons (A)(C) and v'ada neurons (B)(D) under the *dsh/+; Ik2/+*

transheterozygous mutant backgrounds. (E,F) Quantitative analysis of dendrite

severing defects in ddaC neurons (E) and v'ada neurons (F) under the *dsh/+;*

kat-60L1/+ transheterozygous mutant backgrounds. (G,H) Quantitative analysis of

dendrite severing defects in ddaC neurons (G) and v'ada neurons (H) under the *dsh/+;*
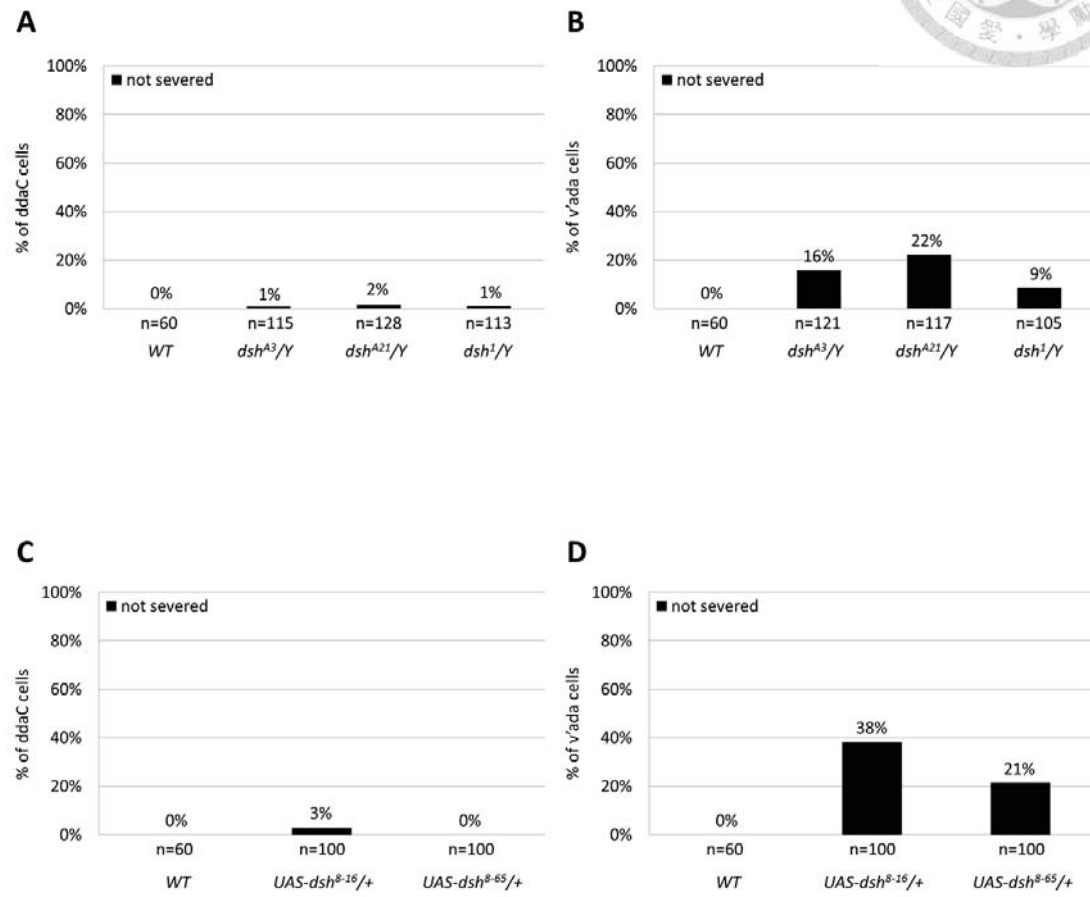
Spn-F/+ transheterozygous mutant backgrounds. The percentages of ddaC/v'ada cells

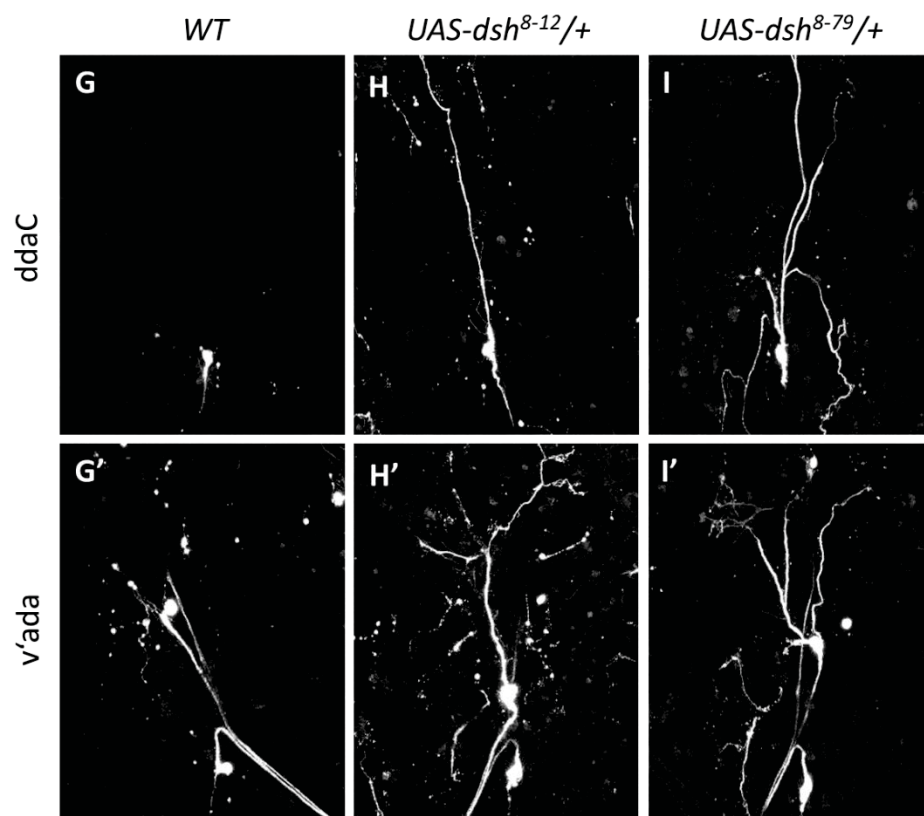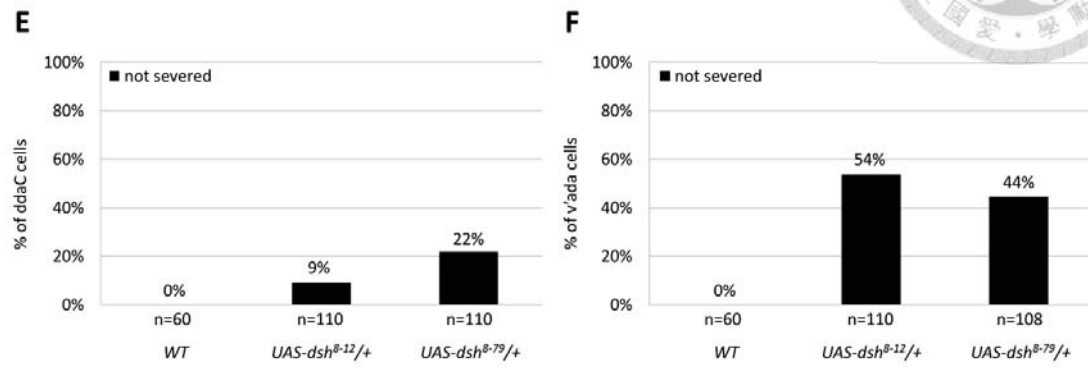represent the number of unsevered neurons dividing the number of total ddaC/v'ada

cells, respectively. The number of ddaC/v'ada neurons in each group is indicated

under the bar.

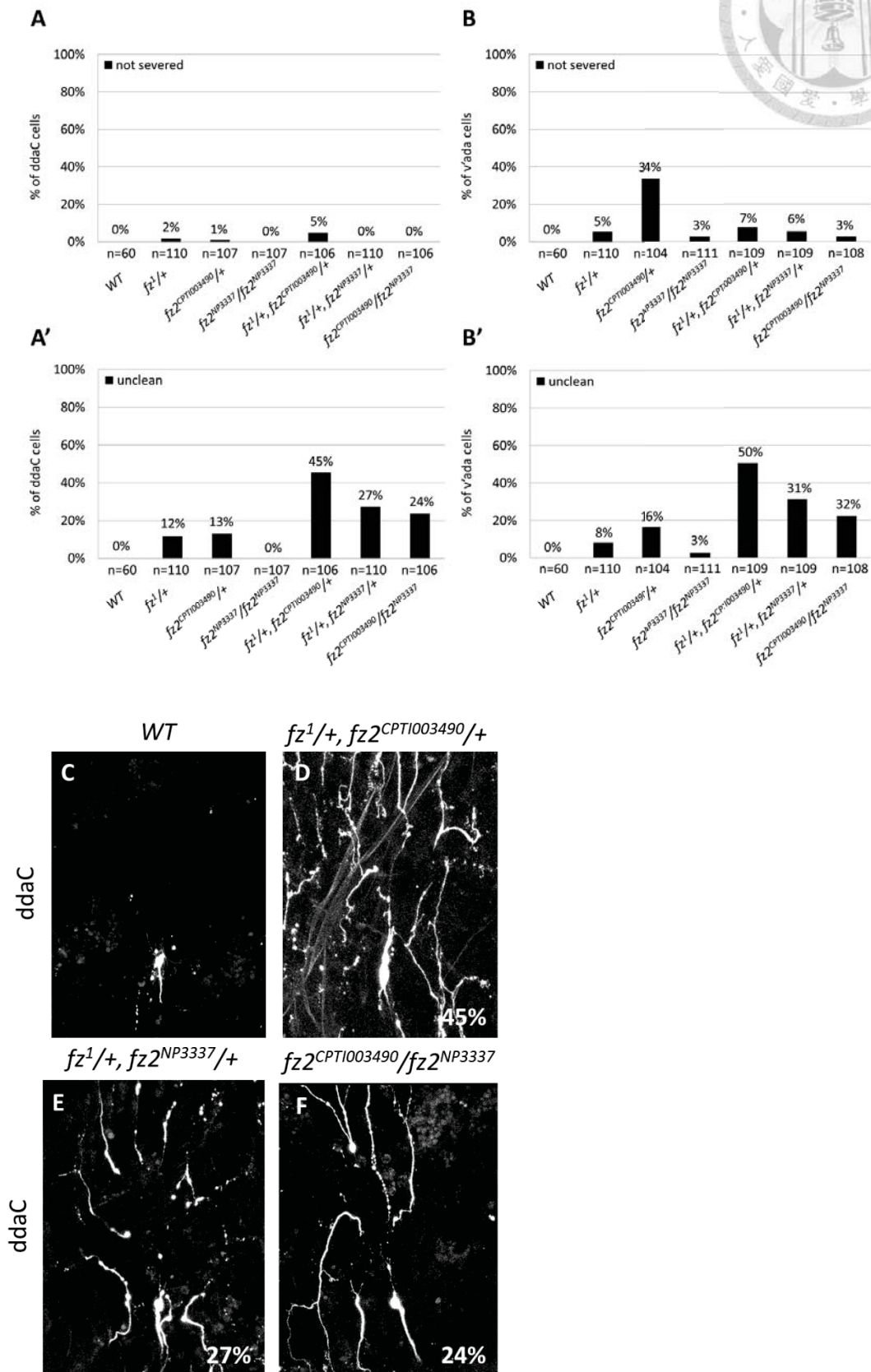# Figure 7

Figure 7 (continued)

Figure 7 (continued)

Figure 7. Mutational analysis of *dsh* with distinct mutated domains showed various morphological changes of dendrite pruning defects

ddaC and v'ada neurons were visualized by expressing *UAS-mCDGFP* driven by *ppk-Gal4* at 16h APF. (A,B) Quantitative analysis of dendrite severing defects in ddaC neurons (A) and v'ada neurons (B) under the DEP-domain-mutated *dsh* backgrounds. (C,D) Quantitative analysis of dendrite severing defects in ddaC neurons (C) and v'ada neurons (D) under the DIX-domain-mutated *dsh* expression backgrounds. (E,F) Quantitative analysis of dendrite severing defects in ddaC neurons (E) and v'ada neurons (F) under the PR-domain-mutated *dsh* expression backgrounds. (G) ddaC neurons and (G') v'ada neurons of *WT*. (H,I) Dendrite severing defects were observed in (H) ddaC neurons and (H') v'ada neurons of *UAS-dsh^{8-12}*/+ mutant and in (I) ddaC neurons and (I') v'ada neurons of *UAS-dsh^{8-79}*/+ mutant. The percentages of ddaC/v'ada cells represent the number of unsevered neurons dividing the number of total ddaC/v'ada cells, respectively. The number of ddaC/v'ada neurons in each group is indicated under the bar.

Figure 8

A

not severed

% of ddaC cells

0% 2% 1% 0% 5% 0% 0%
n=60 n=110 n=107 n=107 n=106 n=110 n=106

WT $fz^1/+$ $fz2^{CPTI003490}/+$ $fz2^{NP3337}/fz2^{NP3337}$ $fz^1/+, fz2^{CPTI003490}/+$ $fz^1/+, fz2^{NP3337}/+$ $fz2^{CPTI003490}/fz2^{NP3337}$

B

not severed

% of v'ada cells

0% 5% 34% 3% 7% 6% 3%
n=60 n=110 n=104 n=111 n=109 n=109 n=108

WT $fz^1/+$ $fz2^{CPTI003490}/+$ $fz2^{NP3337}/fz2^{NP3337}$ $fz^1/+, fz2^{CPTI003490}/+$ $fz^1/+, fz2^{NP3337}/+$ $fz2^{CPTI003490}/fz2^{NP3337}$

A'

unclean

% of ddaC cells

0% 12% 13% 0% 45% 27% 24%
n=60 n=110 n=107 n=107 n=106 n=110 n=106

WT $fz^1/+$ $fz2^{CPTI003490}/+$ $fz2^{NP3337}/fz2^{NP3337}$ $fz^1/+, fz2^{CPTI003490}/+$ $fz^1/+, fz2^{NP3337}/+$ $fz2^{CPTI003490}/fz2^{NP3337}$

B'

unclean

% of v'ada cells

0% 8% 16% 3% 50% 31% 32%
n=60 n=110 n=104 n=111 n=109 n=109 n=108

WT $fz^1/+$ $fz2^{CPTI003490}/+$ $fz2^{NP3337}/fz2^{NP3337}$ $fz^1/+, fz2^{CPTI003490}/+$ $fz^1/+, fz2^{NP3337}/+$ $fz2^{CPTI003490}/fz2^{NP3337}$

WT | $fz^1/+, fz2^{CPTI003490}/+$

C ddaC

D ddaC 45%

$fz^1/+, fz2^{NP3337}/+$ | $fz2^{CPTI003490}/fz2^{NP3337}$

E ddaC 27%

F 24%

Figure 8 (continued)

Figure 8. Mutants of two redundant Wnt receptors, *fz* and *fz2*, showed little dendrite severing defects

ddaC and v'ada neurons were visualized by expressing *UAS-mCDGFP* driven by *ppk-Gal4* at 16h APF. (A,B) Quantitative analysis of dendrite severing defects in ddaC neurons (A) and v'ada neurons (B) and unclean phenotypes in ddaC neurons (A') and v'ada neurons (B') under the *fz* mutant, *fz2* mutant, and *fz/+; fz2/+* transheterozygous mutant backgrounds as indicated. (C) ddaC neurons of *WT*. (D-F) ddaC neurons showed severe un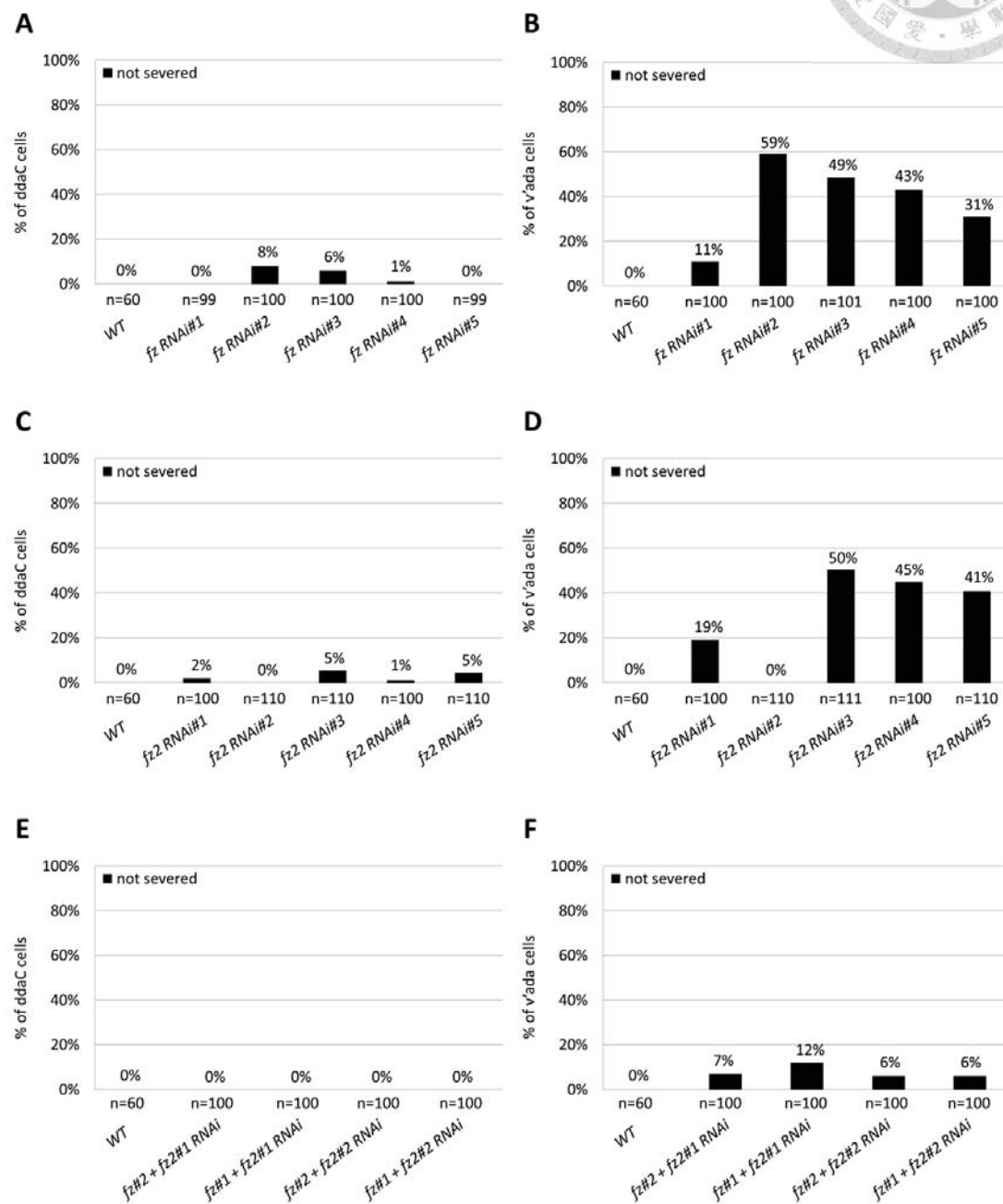clean phenotype of *fz^1/+, fz2^{CPTI003490}/+* (D), *fz^1/+, fz2^{NP3337}/+* (E), and *fz2^{CPTI003490}/fz2^{NP3337}* (F) transheterozygous mutants. The percentages of ddaC/v'ada cells represent the number of unsevered neurons dividing the number of total ddaC/v'ada cells, respectively. The number of ddaC/v'ada neurons in each group is indicated under the bar.
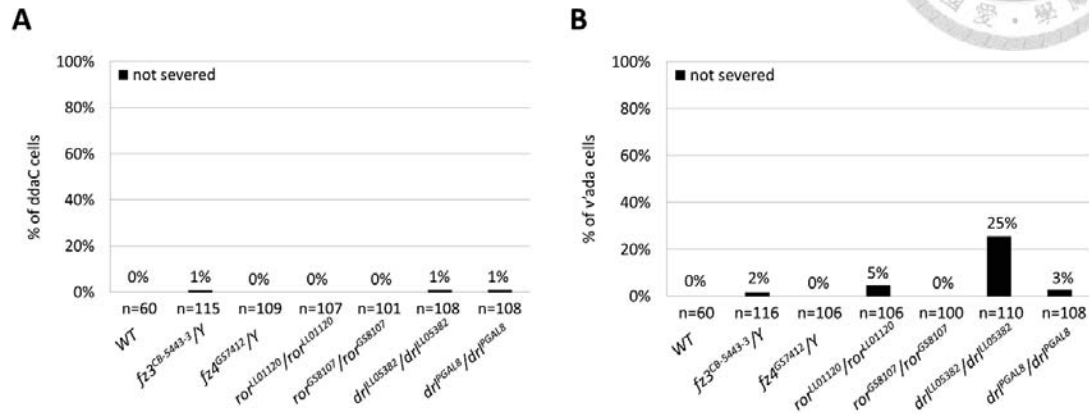
Figure 9

Figure 9 (continued)

Figure 9. Single or double Knockdown of *fz* and *fz2* showed little dendrite severing defects

ddaC and v'ada neurons were visualized by expressing *UAS-mCDGFP* driven by *ppk-Gal4* at 16h APF. (A,B) Quantitative analysis of dendrite severing defects in ddaC neurons (A) and v'ada neurons (B) under the *fz RNAi* backgrounds. (C,D) Quantitative analysis of dendrite severing defects in ddaC neurons (C) and v'ada neurons (D) under the *fz2 RNAi* backgrounds. (E,F) Quantitative analysis of dendrite severing defects in ddaC neurons (E) and v'ada neurons (F) under the *fz* and *fz2* double knockdown backgrounds. The percentages of ddaC/v'ada cells represent the number of unsevered neurons dividing the number of total ddaC/v'ada cells, respectively. The number of ddaC/v'ada neurons in each group is indicated under the bar.
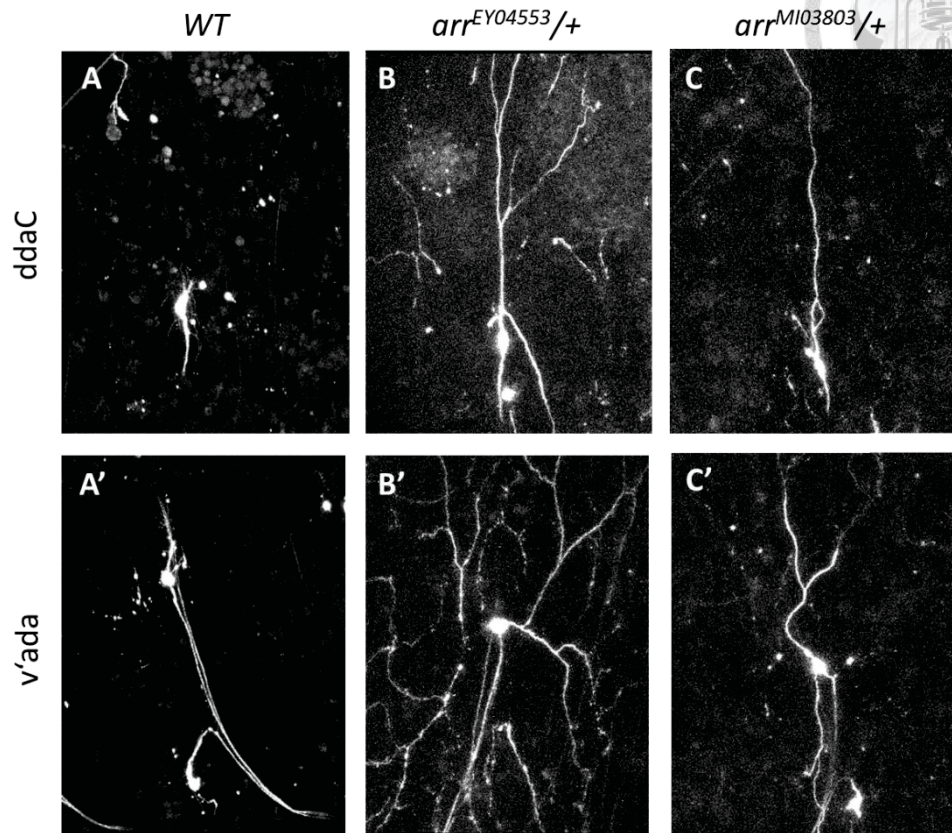
Figure 10

Figure 10. Other receptors involved in multiple Wnt pathways

ddaC and v'ada neurons were visualized by expressing *UAS-mCDGFP* driven by

ppk-Gal4 at 16h APF. (A,B) Quantitative analysis of dendrite severing defects in

ddaC neurons (A) and v'ada neurons (B) under the *fz3*, *fz4*, *ror*, and *drl* mutant

backgrounds as indicated. The percentages of ddaC/v'ada cells represent the number

of unsevered neurons dividing the number of total ddaC/v'ada cells, respectively. The

number of ddaC/v'ada neurons in each group is indicated under the bar.

Figure 11

Figure 11. Mutational analysis of Wg co-receptor *arrow* showed some dendrite pruning defects

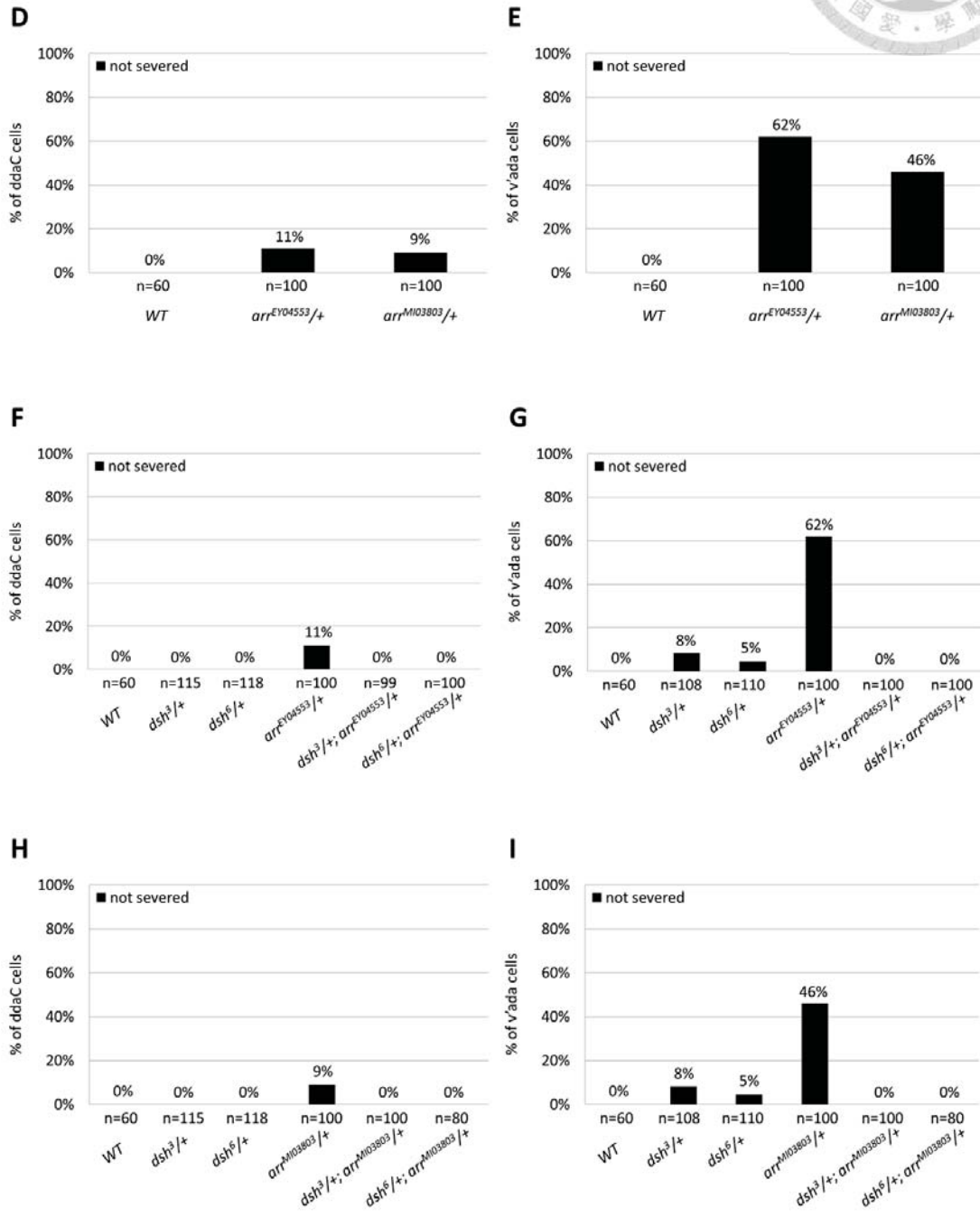ddaC and v'ada neurons were visualized by expressing *UAS-mCDGFP* driven by *ppk-Gal4* at 16h APF. (A) ddaC neurons and (A') v'ada neurons of *WT*. (B,C) Dendrite severing defects were observed in (B) ddaC neurons and (B') v'ada neurons of *arr^{EY04553}*/+ heterozygous mutant and in (C) ddaC neurons and (C') v'ada neurons of *arr^{MI03803}*/+ heterozygous mutant.

Figure 11 (continued)

Figure 11 (continued)

Figure 11. Mutational analysis of Wg co-receptor *arr* showed some dendrite pruning defects

(D,E) Quantitative analysis of dendrite severing defects in ddaC neurons (D) and v'ada neurons (E) under the *arr/+* heterozygous mutant backgrounds. (F-I) Quantitative analysis of dendrite severing defects in ddaC neurons (F) and v'ada neurons (G) under the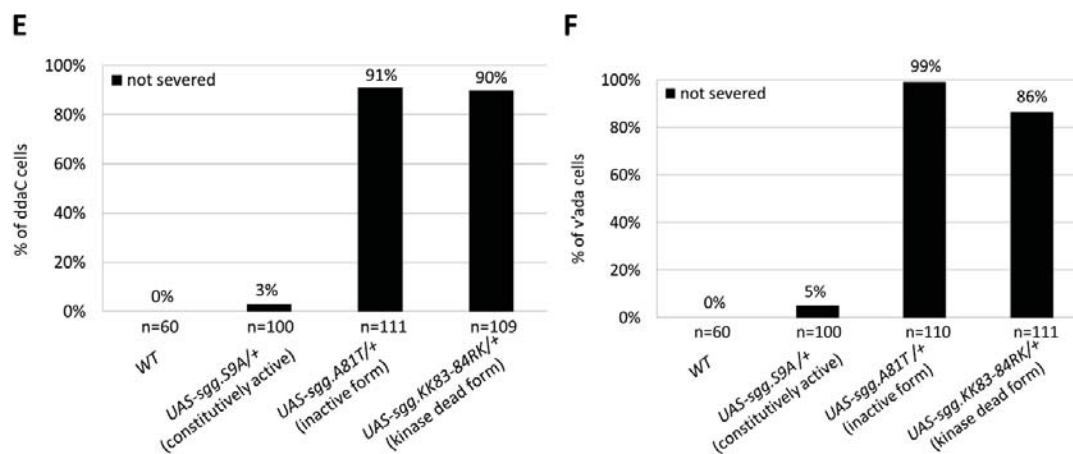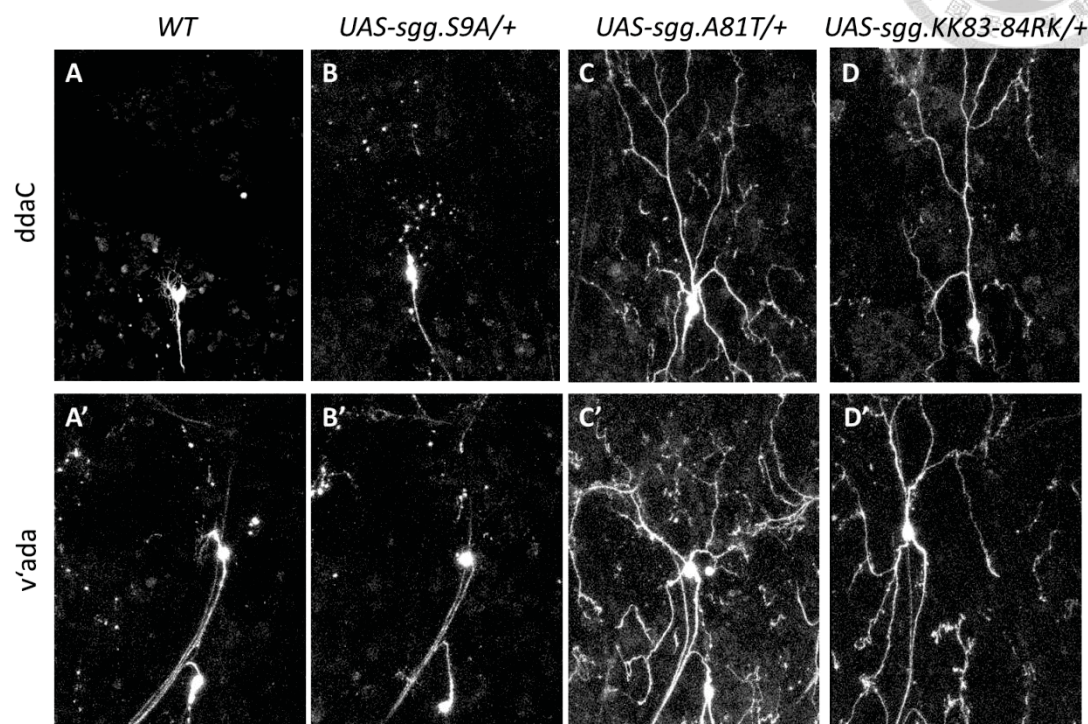 *dsh/+; arr/+* transheterozygous mutant backgrounds. The percentages of ddaC/v'ada cells represent the number of unsevered neurons dividing the number of total ddaC/v'ada cells, respectively. The number of ddaC/v'ada neurons in each group is indicated under the bar.

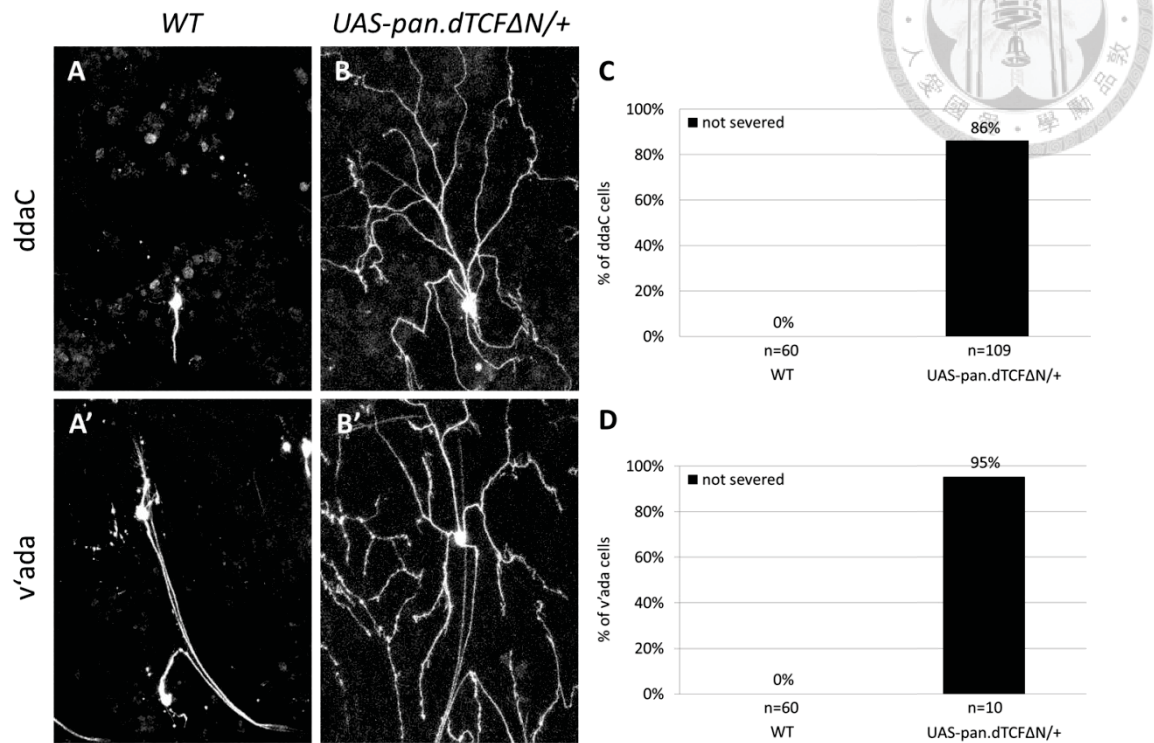# Figure 12

Figure 12 (continued)

Figure 12. Expression of various mutant forms of *sgg* caused severe dendrite pruning defects

(A) ddaC neurons and (A') v'ada neurons of *WT*. (B-D) Dendrite severing defects were observed in (B) ddaC neurons and (B') v'ada neurons of *UAS-sgg.S9A/+*, in (C) ddaC neurons and (C') v'ada neurons of *UAS-sgg.A81T/+*, and in (D) ddaC neurons and (D') v'ada neurons of *UAS-sgg.KK83-84RK/+*. (E,F) Quantitative analysis of dendrite severing defects in ddaC neurons (E) and v'ada neurons (F) under the mutated *sgg* expression backgrounds. The percentages of ddaC/v'ada cells represent the number of unsevered neurons dividing the number of total ddaC/v'ada cells, respectively. The number of ddaC/v'ada neurons in each group is indicated under the bar.

Figure 13

Figure 13. Expression of N-terminal-deletion *TCF* caused critical dendrite severing defects

ddaC and v'ada neurons were visualized by expressing *UAS-mCDGFP* driven by *ppk-Gal4* at 16h APF. (A) ddaC neurons and (A') v'ada neurons of *WT*.

Dendrite severing defects were observed in (B) ddaC neurons and (B') v'ada neurons of *UAS-pan.dTCFΔN/+*. (C,D) Quantitative analysis of dendrite severing defects in ddaC neurons (C) and v'ada neurons (D) under the *dTCFΔN* expression backgrounds.

The percentages of ddaC/v'ada cells represent the number of unsevered neurons dividing the number of total ddaC/v'ada cells, respectively. The number of ddaC/v'ada neurons in each group is indicated under the bar.

78